Cho *et al. Energy Mater* 2024;4:400013
DOI: 10.20517/energymater.2023.72

Energy Materials

Review

Open Access

Check for updates

Advancements in two-dimensional covalent organic framework nanosheets for electrocatalytic energy conversion: current and future prospects

Jin Hyuk Cho[1,#], Youngho Kim[1,#], Hak Ki Yu[2,*], Soo Young Kim[1,*]

[1]Department of Materials Science and Engineering, Korea University, Seoul 02841, Republic of Korea.
[2]Department of Materials Science and Engineering and Department of Energy Systems Research, Ajou University, Suwon 16499, Republic of Korea.
[#]Authors contributed equally.

Correspondence to: Prof. Hak Ki Yu, Department of Materials Science and Engineering and Department of Energy Systems Research, Ajou University, 206 Worldcup-ro, Suwon 16499, Republic of Korea. E-mail: hakkiyu@ajou.ac.kr; Prof. Soo Young Kim, Department of Materials Science, Korea University, 145 Anam-ro, Seongbuk-gu, Seoul 02841, Republic of Korea. E-mail: sooyoungkim@korea.ac.kr

How to cite this article: Cho JH, Kim Y, Yu HK, Kim SY. Advancements in two-dimensional covalent organic framework nanosheets for electrocatalytic energy conversion: current and future prospects. *Energy Mater* 2024;4:400013. https://dx.doi.org/10.20517/energymater.2023.72

Received: 11 Sep 2023 **First Decision:** 9 Nov 2023 **Revised:** 29 Nov 2023 **Accepted:** 11 Dec 2023 **Published:** 19 Feb 2024

Academic Editor: Yun Zhang **Copy Editor:** Fangyuan Liu **Production Editor:** Fangyuan Liu

Abstract

Humanity is confronting significant environmental issues due to rising energy demands and the unchecked use of fossil fuels. Thus, the strategic employment of sustainable and environmentally friendly energy sources is becoming increasingly vital. Additionally, addressing challenges, such as low reactivity, suboptimal energy efficiency, and restricted selectivity, requires the development of innovative catalysts. Two-dimensional (2D) covalent organic frameworks (COFs), known for their limitless structural versatility, are proving to be important materials in energy conversion applications. The exceptional properties of 2D COFs, including an organized arrangement resulting in well-defined active sites and π-π stacking interactions, enable breakthroughs in sustainable energy conversion applications. In this study, we comprehensively investigate universal synthesis methods and specific techniques, such as membrane-based deposition, liquid-phase intercalation, and polymerization. Furthermore, we demonstrate energy-conversion applications of 2D COFs as eco-friendly catalysts for electrochemical processes to promote sustainability and scalability by utilizing them in the hydrogen evolution reaction, oxygen evolution reaction, oxygen reduction reaction, and carbon dioxide reduction reaction. Additionally, we will explore methods for analyzing the physicochemical properties of precisely fabricated 2D COFs. Despite extensive research pertaining to 2D COFs, their practical industrial applications remain limited. Therefore, we

propose various perspectives, including enhancing performance, improving synthesis methods, developing binder-free catalysts, expanding catalyst functionality, and advancing full-cell research, to achieve complete industrialization by leveraging their potential.

Keywords: Covalent organic frameworks, two-dimensional materials, synthesis approach, analytical techniques, energy conversion, electrocatalysts

INTRODUCTION

Human civilization has progressed rapidly and significantly, with no indicator of deceleration in the foreseeable future. To sustain and further propel this progress, the amount of energy supply must be increased[1]. However, the predominant reliance on fossil fuels, which currently constitute the largest proportion of energy sources, presents not only the challenge of limited energy resources but also detrimental consequences caused by significant carbon dioxide (CO_2) emission during combustion, thus exacerbating global warming[2,3]. Consequently, sustainable and environmentally friendly alternative energy conversion methods are urgently required[4-6]. Considering the constraints posed by the limited conditions and low energy efficiency of renewable energy generation, the integration of catalysts has emerged as a promising solution to address these challenges and foster a sustainable energy future[7]. Significant advancements can be realized to enhance the efficiency and effectiveness of renewable energy conversion processes by leveraging catalytic properties, including those of transition metal dichalcogenides[8,9], transition metal chalcogenides[10], metal-organic frameworks (MOFs)[11], and covalent organic frameworks (COFs)[12,13]. These materials provide a substantial active surface area owing to their high surface-to-volume ratio, which facilitates efficient interactions and enhances the catalytic performance. Moreover, their tunable electronic properties enable catalyst optimization, thus allowing precise control over the catalytic activity, selectivity, and stability through composition and layer stacking strategies[14,15]. In particular, COFs have been investigated continuously since their initial introduction in 2005[16]. As porous materials composed of interconnected organic building blocks formed by covalent bonds, they possess a unique advantage: their exceptional ability for precise structural manipulation enables the creation of tailor-made designs customized to suit specific applications, a distinction that sets them apart from conjugated microporous polymers (CMPs)[17] and hierarchically porous carbons (HCPs)[18], primarily characterized by carbon and nitrogen-based porous structures. Numerous types of COFs with distinctive characteristics have been reported, including the bipyridine-based COF[19], which incorporates heteroatomic nitrogen; the triphenylene-based COF[20], which features a well-ordered and regular structural arrangement; the pyrazine-based COF[21], which is well known for its electrochemical stability; and the polydopamine-based COF[22], which is distinguished by its biocompatibility and surface adhesion properties. In addition, COFs offer precise control over composition, pore size, and functionality, along with design flexibility, to accommodate various applications[23].

Within the realm of COFs, the meticulously structured two-dimensional (2D) COFs stand out due to their well-defined active sites and π-π stacking interactions, which contribute to their heightened catalytic activity and enhanced selectivity[24,25]. Compared to their three-dimensional (3D) counterparts, 2D COFs offer superior capabilities in modulating molecular dimensions and crystallinity. This adaptability aids in fine-tuning intermolecular interactions, thus promoting specific reactions[26]. Additionally, the interactions between layers in 2D COFs enhance their electrochemical properties. This enhancement is achieved through activation processes, added functionality, and improved selective adsorption[27]. In this review, we aim to comprehensively elucidate the chemical methodologies employed in the synthesis of 2D COFs through both top-down and bottom-up approaches, along with the utilization of advanced characterization techniques [Scheme 1]. In the characterization section, we focus on two essential analytical techniques:

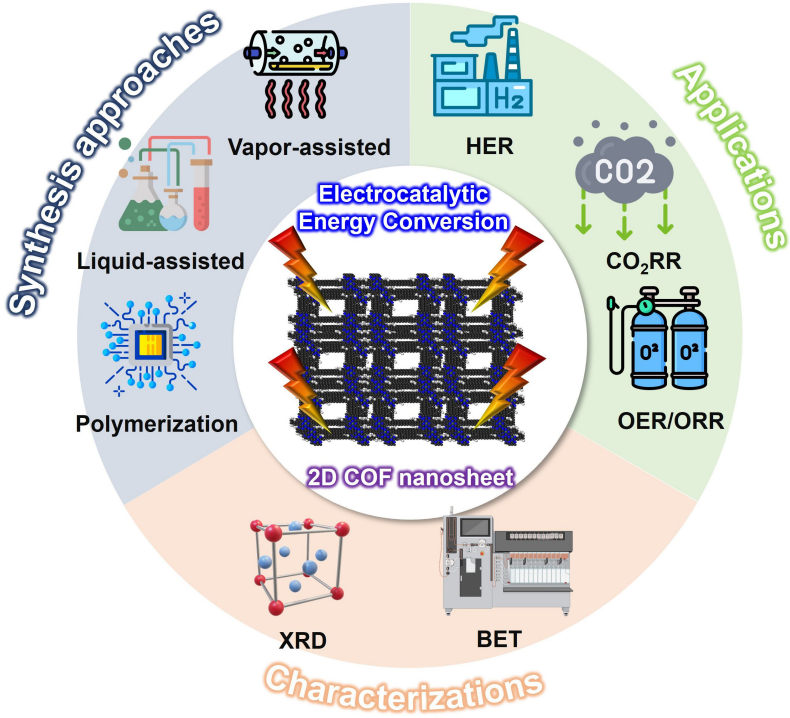

Scheme 1. Schematic representation of synthesis approaches, applications, and characterizations of 2D COF nanosheets.

X-ray diffraction (XRD) and the Brunauer-Emmett-Teller (BET) analysis. XRD reveals the crystal structure and phase composition, thereby offering valuable insights into the atomic arrangement within the material[28,29]. The BET analysis reveals the specific surface area and porosity of the samples, thus providing crucial information regarding their physical properties and potential practical applications[26,30]. Furthermore, we provide illustrative examples of the utilization of 2D COFs as catalysts for energy conversion processes, such as the electrochemical oxygen evolution reaction (OER), oxygen reduction reaction (ORR), hydrogen evolution reaction (HER), and CO_2 reduction reaction (CO_2RR). In various fields of energy conversion, 2D COFs exhibit advantages over 3D COFs, including significant surface area, efficient charge transfer, flexibility, design versatility, and ease of processing. These characteristics facilitate interactions and chemical reactions among specific compounds, thereby enhancing the reaction rates of the catalysts and ensuring selectivity. Finally, we discuss the limitations inherent to 2D COFs and propose potential strategies for overcoming these challenges.

SYNTHESIS APPROACHES

The synthesis of 2D COFs can be classified into top-down and bottom-up methods[31]. Top-down methods entail the precision removal or manipulation of a target material from larger structures, enabling the attainment of the desired nano-scale configuration. In contrast, bottom-up methods encompass the assembly of molecules or atoms through chemical reactions and self-assembly processes to construct large-scale structures[32]. In this study, we aim to provide a comprehensive classification that encompasses both universal and specific synthesis approaches, such as deposition techniques, liquid-phase intercalation, and polymerization, along with their respective procedures.

A wide range of porous organic polymer networks have been classified [Scheme 2], such as crystalline COFs (CCOFs) and various amorphous networks, such as hypercrosslinked polymers (HCPs), covalent triazine frameworks (CTFs), porous aromatic frameworks (PAFs), and CMPs.

Vapor-assisted deposition technique

Chemical vapor-assisted deposition (CVD) techniques are regarded as exceptional synthesis methodologies for controlling the structures and properties of 2D COFs. These techniques exhibit remarkable advantages, including the formation of precise and uniform layers, thus enabling large-scale fabrication and facilitating the creation of diverse material compositions contingent upon deposition or growth conditions. Additionally, they afford meticulous control over the chemical properties (such as the crystallinity, thickness, and other structural characteristics)[38,39]. Moreover, their inherent scalability renders them to be advantageous for industrialization and commercialization, thus enhancing their appeal for developing advanced materials[40]. As shown in Figure 1A, 4,4′,4″,4‴- (PyTTA-TPA), 4,4′,4″,4‴-(1,3,6,8-Tetrakis(4-aminophenyl)pyrene-[2,2′-Bipyridine]-5,5′-dicarboxaldehyde (PyTTA-BPyDCA), and 4,4′,4″,4‴-(1,3,6,8-Tetrakis(4-aminophenyl)pyrene-4,4′-Biphenyldicarboxaldehyde (PyTTA-BPDA) COF films were synthesized using ambient-pressure CVD. The PyTTA monomer was uniformly loaded onto a clean growth substrate through thermal evaporation, thus allowing precise control of the growth thickness[41]. The substrate with PyTTA was placed in a quartz tube inside a tube furnace, whereas TPA powders were placed in a ceramic boat heated to 80 °C. The tube furnace was connected to a bubbler containing an acetic acid solvent, and hydrogen and argon were used as carrier gases to transport H_2O, acetic acid, and TPA vapor for COF synthesis on the PyTTA surface. Increasing the temperature from 80 to 150 °C resulted in faster reactions. Based on meticulous screening, a growth temperature of 140 °C was selected to generate large-area COF films on substrates, which is cost-effective for large-scale COF film production. The 2D COF film fabricated using the vapor-induced conversion method exhibited remarkable efficacy as an electrochemical catalyst for the HER. Additionally, Chaki Roy *et al.* successfully fabricated 2D COFs via CVD, where vapor-induced conversion with PyTTA was used as a pristine precursor[42]. The suggested incorporation of COF366-QD thin films onto a silicon substrate through in-situ low-temperature CVD is promising for promoting progress in the transfer-free and economically viable manufacturing of extensive organic electronics and direct device applications. The structure of the fabricated COF366-QD thin film is shown in Figure 1B. In conclusion, CVD is widely acknowledged as a prominent technique in the production of diverse 2D COFs, primarily because of its inherent benefits, such as high deposition velocity, precise layer control, and the ability to enable large-scale manufacturing.

Liquid-assisted synthesis method

In this section, we discuss solvent absorption[43], insertion[44], infiltration[45], encapsulation[46], and solvothermal processes[47], with specific focus on their application in the liquid-phase synthesis of 2D COFs. Solvent absorption involves the permeation of solvent molecules into the internal structure of a material, which effectively fills the internal voids[48]. This approach enables the alteration of material properties or imparts new characteristics by leveraging solid-liquid interactions. Kang *et al.* investigated four distinct 2D COFs: 1,3,5-tris(4-aminophenyl)benzene-terephthalaldehyde (TAPB-TA); 1,3,5-tris(4-aminophenyl)benzene- 2,5-dimethoxyterephthalaldehyde (TAPB-OMeTA); 4,4′,4″,4‴-(1,9-dihydropyrene-1,3,6,8-tetrayl)tetraaniline-terephthalaldehyde (Py-1P), and 2,4,6-tris(4-aminophenyl)-1,3,5-triazine-benzene-1,3,5-tricarbaldehyde (TAPT-BTCA), using the solvation method[49]. Their investigation revealed a significant interlayer-shifting phenomenon in these COFs when exposed to solvents, which resulted in significant changes to their stacking structures. This remarkable flexibility demonstrated by the TAPB-TA, TAPB-OMeTA, Py-1P, and TAPT-BTCA COFs facilitates the accurate determination of the structure of solvated COFs, which requires advanced analysis techniques such as powder XRD (PXRD), simulation modeling, and Pawley refinement. The synthesis of the 2D COFs is illustrated in Figure 2A. Solvothermal

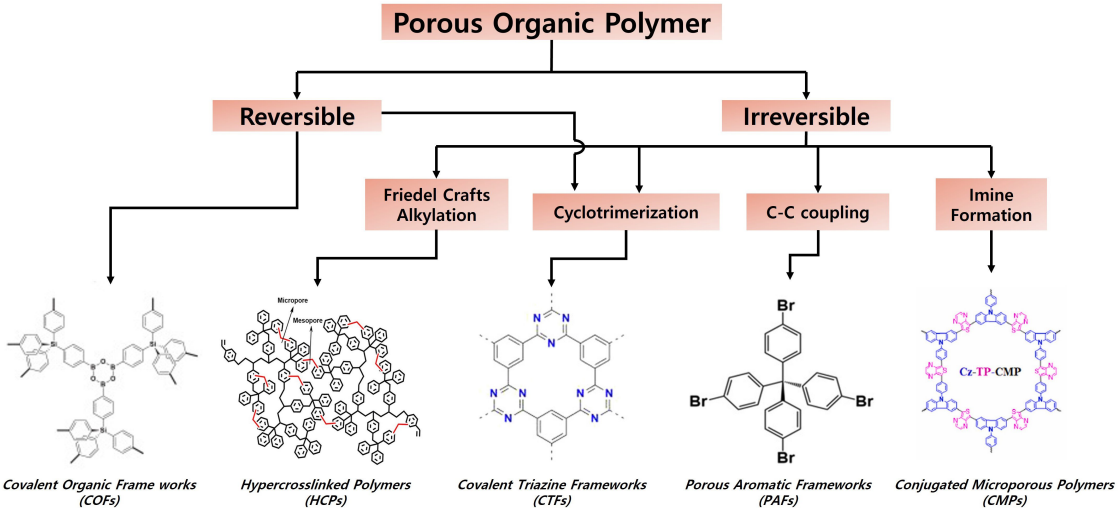

Scheme 2. Types of porous organic polymer frameworks and their coupling chemistries. Porous polymers from left to right: COFs. Reproduced with permission. Copyright 2021, Elsevier[33]. HCPs. Reproduced with permission. Copyright 2021, Elsevier[34]. CTFs. Reproduced with permission. Copyright 2013, American Chemical Society[35]. PAFs. Reproduced with permission. Copyright 2020, American Chemical Society[36]. Conjugated CMPs. Reproduced with permission. Copyright 2022, Elsevier[37].

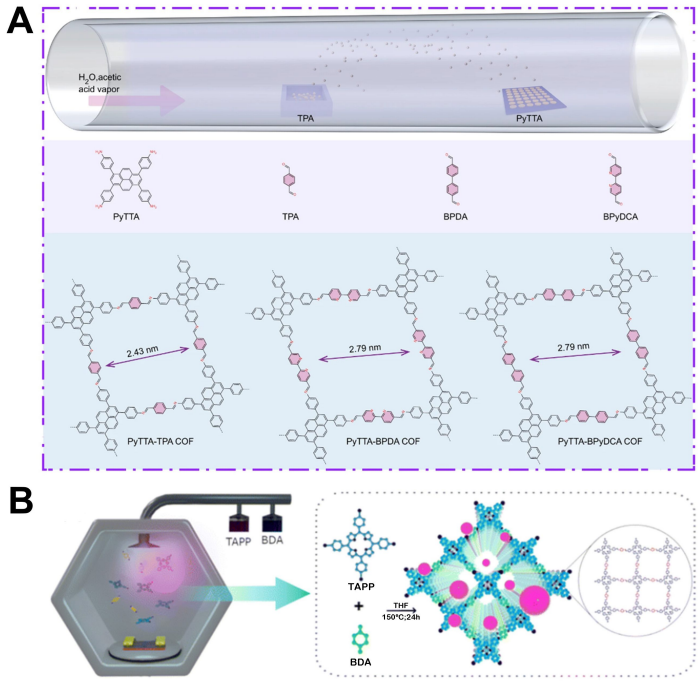

Figure 1. (A) Schematic representation of growth of imine-linked 2D COF films on SiO_2/Si substrates. Reproduced with permission. Copyright 2022, Springer Nature[41]. (B) Schematic illustration of in-situ low-temperature CVD equipment setup and final structural model of COF366-QD thin films. Reproduced with permission. Copyright 2023, Royal Society of Chemistry[42].

synthesis is the predominant method utilized for the fabrication of 2D COFs, and the solvent employed in this process assumes several pivotal roles[50]. (1) The solvent enhances the solubility of the reactants, thereby facilitating improved mixing and interactions between them; (2) The solvent can control the temperature and pressure, thereby facilitating the establishment of targeted reaction conditions and the precise regulation of reaction kinetics; and (3) The solvent contributes significantly to the growth and crystallization of the resulting material, thereby affecting the desired physical and chemical properties.

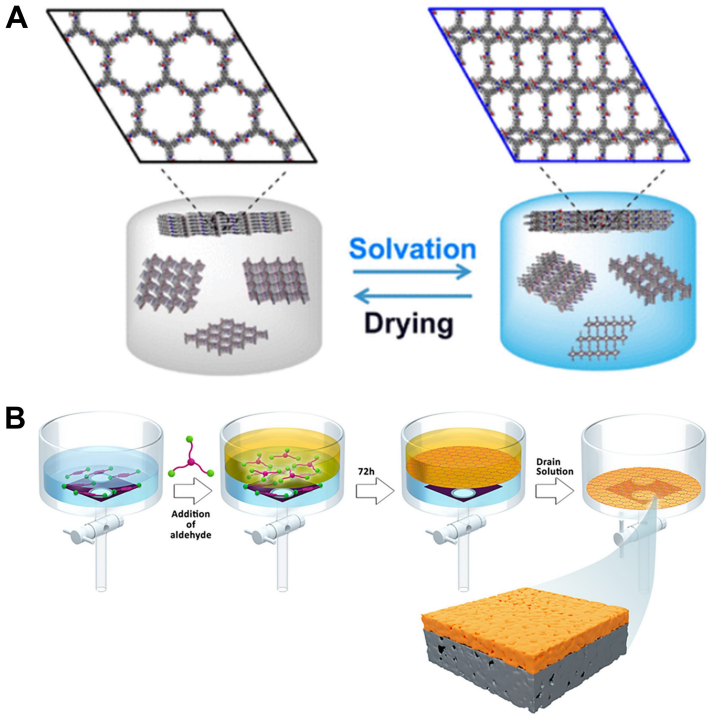

Figure 2. (A) Schematic illustration of 2D COF synthesis processes based on solvation method. Reproduced with permission. Copyright 2020, American Chemical Society[49]. (B) Synthesis process of large-scale nanoporous 2D COF membranes. Reproduced with permission. Copyright 2022, American Chemical Society[51].

Hence, the solvent used in solvothermal synthesis determines the morphology and characteristics of the desired material. Shevate *et al.* proposed a modified Langmuir method and incorporated solvothermal synthesis to fabricate large-area 2D COF membranes with adjustable nanopore sizes [Figure 2B][51]. In addition, Ji *et al.* reported that weakly CCOFs undergo temperature-dependent depolymerization during synthesis, thus further highlighting the potential for improving material quality through repeated depolymerization and repolymerization cycles[52]. Additionally, researchers have investigated solvothermal depolymerization and recrystallization methods to control COF formation and enhance material quality. These processes are similar to molecular recrystallization and provide valuable insights into the formation of imine-linked 2D COFs, thus presenting a novel approach for improving the crystallinity of COFs. Xu *et al.* developed two flexible 2D COFs, namely TPT-COF-1 and TPT-COF-2, using triaryloxytriazine molecules as building blocks[53]. These triaryloxytriazines exhibit intriguing trigonal structures characterized by π stacking and weak hydrogen bonding strands. These 2D COFs were synthesized via a solvothermal method on a gram scale, which resulted in the formation of highly crystalline materials with large surface areas. Notably, this approach yields COFs that are different from previously reported COFs, which are typically synthesized at the microgram scale.

Polymerization

Polymerization is a process that involves covalently linking fundamental building blocks to generate extensive molecular chains[54]. As the reaction progresses, bonding occurs and is affected by the surrounding environment, thus resulting in intricate 2D COF architectures. Precise optimization can be achieved by judiciously regulating factors such as the reaction rate, bonding robustness, and structure formation. Polymerization occurs intrinsically during the previously mentioned synthesis methods, where chemical bond formation is catalyzed, thus expediting the overall reaction[55]. This process is particularly important in the COF synthesis pathway and warrants further investigation. Yang *et al.* successfully fabricated 2D COF membranes with outstanding solvent resistance via interfacial polymerization. They overcame the

challenges encountered in previous methodologies to enhance the chemical resistance of polymeric substrates by adopting an innovative approach[56]. As depicted in Figure 3A, the detailed synthesis method involves the carbonization of commercial polyacrylonitrile (PAN) ultrafiltration membranes under an inert atmosphere while incorporating calcium nitrate as a pore-forming agent. This process yielded carbonized PAN substrates featuring crosslinked structures while maintaining finger-like pores with sizes ranging from 100 to 500 nm. Furthermore, these substrates demonstrated exceptional scalability and foldability without adverse effects. Subsequently, in-situ interfacial polymerization was adopted to synthesize interconnected 2D COF membranes on carbonized PAN substrates, where an aldehyde monomer of 1,3,5-triformylphloroglucinol (Tp) and the following four distinct amine monomers were used: hydrazine hydrate (HZ), 1,3,5-tris(4-aminophenyl)benzene (TAPB), p-phenylenediamine (PDA), and 3,3-dihydroxybenzidine (DHBD). Consequently, they successfully created distinct COF membranes designated as Tp-HZ, Tp-TAPB, Tp-PDA, and Tp-DHBD. Zhan *et al.* conducted a comprehensive examination of polymerization and crystallization to fabricate well-defined crystalline 2D polymers at the solid-liquid interface under ambient conditions[57]. By utilizing state-of-the-art in-situ scanning tunneling microscopy, they obtained valuable insights into the intricate processes. The solid-liquid interface provides a significant advantage by effectively decoupling 2D polymerization from the stacking/destacking processes, which is crucial in the formation of 2D COFs. The self-condensation of pyrene-2,7-diboronic acid (PDBA) was investigated to synthesize various 2D COF structures through dynamic covalent chemistry. Interfacial polymerization for 2D COF synthesis encompasses a range of synthesis methods beyond the solid-liquid approach previously discussed. The choice of method varies, depending on specific applications and requirements. These methods include: (1) Solid-vapor interface: This approach offers the advantage of simply increasing the temperature to accelerate the reaction rate, resulting in higher-quality 2D COF membranes and decreased membrane thickness[58]; (2) Liquid-air interface: This approach enables the fabrication of large-area COF membranes and demonstrates excellent performance in electrochemical reactions due to its high availability[59]; and (3) Liquid-liquid interface: This approach demonstrates remarkable versatility, enabling a diverse spectrum of polymerization reactions by amalgamating two distinct liquid-phase reactants[60]. Evans *et al.* introduced a novel polymerization approach based on the 90 °C sequence solvothermal technique and incorporated two seeded growth steps [Figure 3B][61]. This innovative method offers a versatile and modular approach for generating high-quality 2D polymers via directional bonding. In a specific synthesis process, COF-5 nanoparticles were initially formed through the solvothermal condensation of 1,4-phenylenebis(boronic acid) and 2,3,6,7,10,11-hexahydroxytriphenylene in a mixture comprising 1,4-dioxane and mesitylene. Subsequently, the monomer concentration was controlled by gradually introducing additional monomers into the reaction mixture, which resulted in controlled colloidal growth. Finally, the results of these exploratory experiments demonstrated the successful synthesis of high-quality COF-5 nanoparticles, which measured between 30 to 400 nm.

Other synthesis methods

In the realm of 2D COF synthesis, "exfoliation" typically refers to delicately separating pre-formed thick 2D COF layers into thinner, individual layers[62]. This is essential for reducing the thickness of 2D COFs and obtaining layered structures that exhibit exceptional properties tailored for specific applications[63]. Furthermore, exfoliation can extend its scope beyond simply thinning thick layers and encompass the process of forming more complex material structures[64]. To apply exfoliation to 2D COFs, one must disrupt the interlayer interactions. However, exfoliation is not universally applicable to all 2D COFs because its success depends on the structure and characteristics of the synthesized material. The presynthesized microcrystalline COF-43 powder, which was prepared via solvothermal synthesis, was purified thoroughly to ensure the complete removal of residual substances [Figure 4A][65]. Meanwhile, the results of atomic force microscopy (AFM) analysis demonstrated that COF-43 subjected to sonication with dioxane exhibited significantly reduced average heights (1.32 nm) as compared with COF-43 treated with THF [Figure 4B].

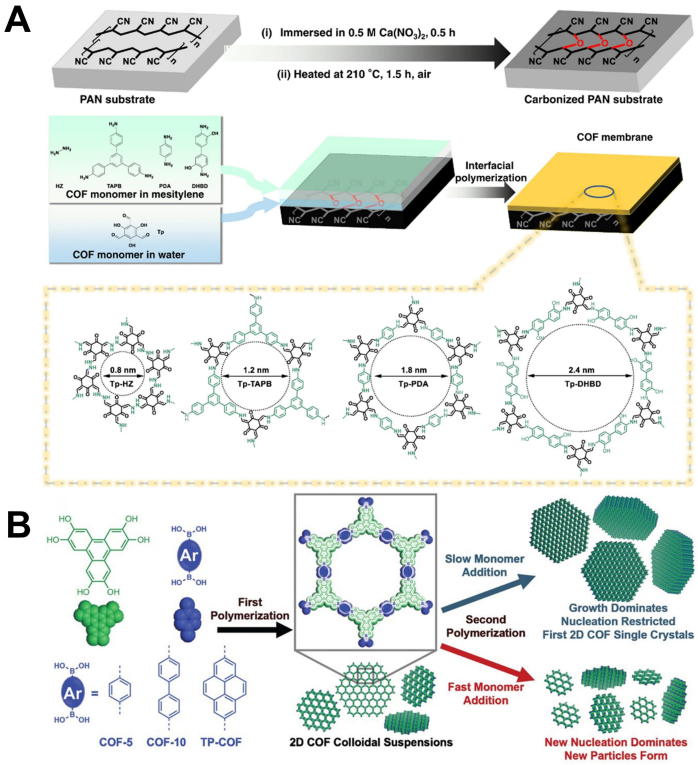

Figure 3. (A) Schematic diagram illustrating carbonization processes of PAN substrates and the subsequent interfacial polymerization with various monomers to fabricate 2D COF membranes. Reproduced with permission. Copyright 2023, Springer Nature[56]. (B) Schematic diagram illustrating two-step polymerization processes for fabrication of high-quality 2D COFs. Reproduced with permission. Copyright 2018, The American Association for the Advancement of Science[61].

This finding strongly implies the formation of a single-layer structure in the dioxane-sonicated COF-43. In addition, the incorporation of an in-situ linker exchange by Zhang *et al.* is a novel strategy for customizing the properties of 2D COFs[66]. Through the deliberate substitution of molecular linkers within existing frameworks, 2D COFs with precise attributes suitable for diverse applications can be customized and synthesized. As shown in Figure 4C, heterostructured 2D COF membranes were successfully engineered via an in-situ linker exchange approach, wherein a fraction of ACOF-1 was substituted with COF-LZU1. Figure 4D shows a schematic illustration of the stepwise structural transformation of the 2D COF membrane.

CHARACTERIZATIONS

XRD analysis

XRD is a highly valuable analytical technique that is widely employed for elucidating material structures and properties; furthermore, it is used extensively to analyze the crystallinity of 2D COFs[28,29,67]. Because of the ordered crystalline structures of 2D COFs, XRD allows one to investigate their molecular alignments and interactions and precisely determine their intermolecular spacing. Moreover, the evaluation of the crystal quality, which directly affects the functional properties of 2D COFs, enables the optimization of manufacturing processes[68]. By monitoring the changes in 2D COF crystal structures under diverse conditions, valuable insights into the stability and physical characteristics, along with the analysis of defects, can be gained. Therefore, XRD provides essential information regarding the structure, crystal quality, lattice constants, structural transformations, and functional properties of 2D COFs, thereby contributing significantly to the development and utilization of these materials[69]. Mahmood *et al.* fabricated a 2D COF with a fully conjugated fused aromatic structure featuring aromatic amine (-NH_2) and hydroxyl (-OH)

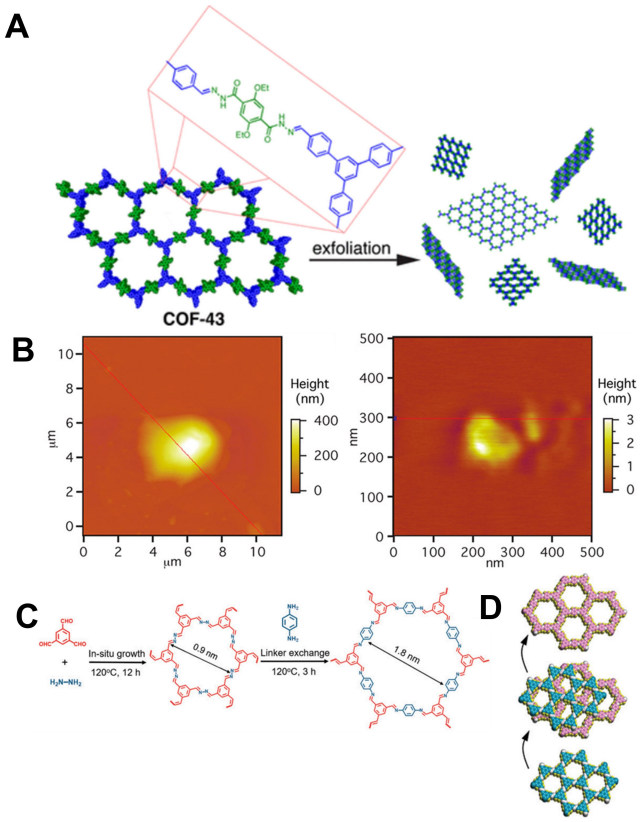

Figure 4. (A) Fabrication process of 2D COF membranes using microcrystalline powder of COF-43 via exfoliation methods. (B) AFM images of 2D COF-43. Left: COF-43 treated with THF; right: COF-43 treated with dioxane. Reproduced with permission. Copyright 2013, American Chemical Society[65]. (C) Schematic diagram illustrating fabrication of heterostructure 2D COFs via in-situ growth and linker exchange methods. (D) Structural transformation of 2D COF membrane as a function of synthesis time. Reproduced with permission. Copyright 2022, Royal Society of Chemistry[66].

functionalities within the pores. In particular, a potent polycondensation process (aromatization) involving pentaaminophenol and hexaketocyclohexane (HKH) in trifluoromethanesulfonic acid was performed[70]. Figure 5A illustrates the confirmed crystalline structure of the synthesized F-COF, which was obtained both experimentally and numerically. The results show that F-COF exhibits a hexagonal arrangement with an AA-stacking model and a layer-to-layer distance of 3.30 Å, which does not align with the ab-stacking model [Figure 5B and C]. Li *et al.* introduced a novel method to prepare imine-linked 2D COF solid solutions by adjusting the ratio of two linear monomers, i.e., PDA and 4,4′-biphenyldicarbaldehyde (BDA)[71]. This innovative approach allows precise control over the monomer feed ratios, thus resulting in enhanced complexity in the composition and structure of 2D COFs. The XRD analysis presented in Figure 5D-F reveals that the (100) diffraction peak remained stable, with a slight shift depending on the BDA monomer ratio (after different synthesis times: 15, 30 min, and 1 h). This shift provides compelling evidence of the successful integration of BDA into the PDA lattice. Cao *et al.* investigated the intriguing phenomenon of membrane polarity switches by employing a sophisticated multivariate approach (COF-V) to adjust the solution pH[72]. This innovative method involves integrating vinyl groups into COFs and facilitating subsequent post-synthesis functionalization through thiol-ene click chemistry while preserving the crystalline structure of the COFs. The initial COF-V membranes were skillfully synthesized on a PAN support via an interfacial condensation reaction, with particular emphasis on the COF-V-60% membrane, which presented significant characterization outcomes. Figure 5G and H show comparisons of the XRD patterns and grazing incidence wide-angle X-ray scattering (GIWAXS) to validate the crystal structures of the COF-V and cysteine-functionalized COF (COF-Cys) membranes at different concentrations.

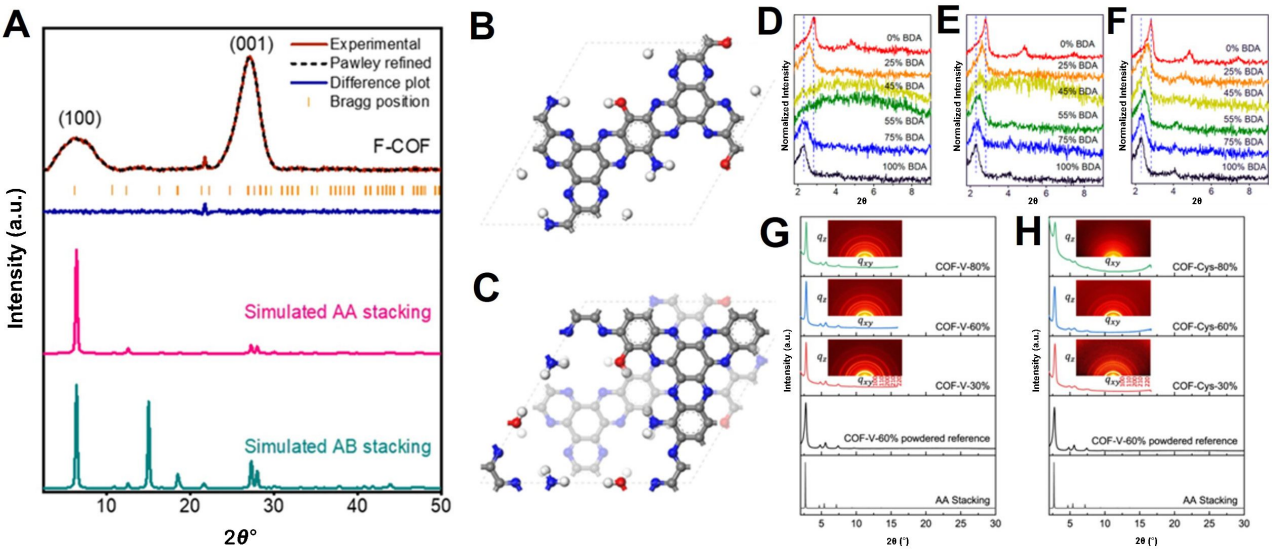

Figure 5. (A) PXRD patterns of F-COF, including Pawley-refined patterns. Atomic model of F-COF with (B) AA stacking structures and (C) AB stacking structures. Reproduced with permission. Copyright 2020, Springer Nature[70]. PXRD patterns of 2D COFs synthesized at various BDA monomer ratios. Synthesis time (D): 15 min (E): 30 min (F): 60 min. Reproduced with permission. Copyright 2021, American Chemical Society[71]. (G) XRD patterns of COF-V-x% (30%, 60%, 80%). Inset: GIWAX patterns (H): XRD patterns of COF-Cys-x% (30%, 60%, 80%). Inset: GIWAX patterns. Reproduced with permission. Copyright 2022, Springer Nature[72].

BET measurement

The large specific surface areas and porosities of 2D COFs are their major advantages, and BET measurements are essential for evaluating these characteristics[73]. To elaborate further, a substantial specific surface area and fine-tuned pore size can lead to an increase in electrocatalytic activity by augmenting the number of active sites, facilitating improved mass transport, and enhancing charge transfer processes[74,75]. Chen *et al.* successfully synthesized stable porphyrin-based 2D COFs containing H_2, Co, Ni, and Zn by preparing porphyrinic aldehyde p-MPor-CHO[76]. Subsequently, they performed a condensation reaction using 2,5-diethoxyterephthalohydrazide (DETH) to obtain MPor-DETH-COFs, as depicted in Figure 6A-D. Figure 6E-H shows that the MPor-DETH-COFs incorporating H_2, Co, Ni, and Zn feature large surface areas, with values of 820, 940, 770, and 1,020 m^2g^{-1}, respectively (with a pore size of approximately 2.4 nm, as shown in the insets of Figure 6E-H). Evans *et al.* prepared boronate-ester-linked 2D COF colloidal inks and performed spray coating to fabricate high-quality 2D COF thin films on substrates, including polymers, metals, and oxides[77]. As shown in Figure 6I and J, the synthesized 2D COFs exhibited large surface areas (reaching 1,900 m^2g^{-1}) and a pore size of 50 nm. This outcome can be attributed to the capability of spray coating to achieve a uniform dispersion of COFs and enable deposition into a thinner layer, thereby facilitating the creation of an enhanced surface structure and micro-porosity. In conclusion, 2D COFs, characterized by their extensive specific surface area as measured by BET, enhance interactions among catalytic particles and sustain stability during prolonged reactions. Moreover, these COFs are notably beneficial for electrochemical transformations due to their ability to enhance interactions among various chemical species.

APPLICATIONS

Catalysts can be classified into several categories: electrocatalysts, photocatalysts[24,25,78,79], thermal catalysts, and photochemical catalysts[80,81]. Among them, electrocatalysts have received significant attention because of their ability to function in various environments. Electrocatalysis involves the use of a catalyst to

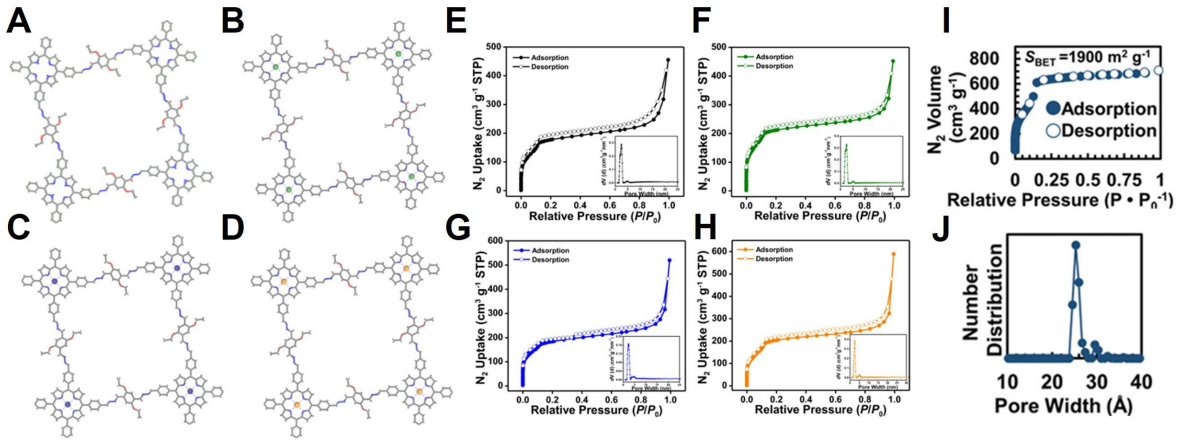

Figure 6. Atomic structure modeling of MPor-DETH-CO (M: H_2, Co, Ni, Zn) (A): H_2 (B): Co (C): Ni (D): Zn BET surface area measurement of MPor-DETH-CO (E): H_2 (F): Co (G): Ni (H): Zn Reproduced with permission. Copyright 2021, Springer Nature[76]. (I) BET measurement and (J) pore size distribution of COF-5 films. Reproduced with permission. Copyright 2020, John Wiley and Sons[77].

accelerate electrochemical reactions and is critical to numerous energy conversion and storage applications, including water splitting[82-84], CO_2 reduction[85,86], fuel cells, and batteries[87,88]. Conventional electrocatalysts typically involve the use of expensive and rare metals, such as platinum and palladium, which limits their widespread adoption. By contrast, 2D COFs offer immense potential for advanced energy conversion and storage applications[89]. 2D COFs possess unique properties and are cost-effective, thus rendering them ideal candidates for overcoming the limitations of conventional catalysts and promoting the development of more sustainable and efficient alternatives[90]. One of the appealing aspects of 2D COFs for electrocatalysis is their modular and customizable features, which allow for the precise control of their structure, pore size, and surface chemistry[91,92]. This enables the customized design and optimization of the catalyst properties. Moreover, the well-defined and ordered pores within 2D COFs enhance mass transport, facilitating the diffusion of reactants and, hence, improving catalytic performance.

In electrocatalysis, 2D COFs can serve as efficient catalysts or support materials for other catalytic species[93]. For example, 2D COFs can be functionalized with specific catalytic sites, such as metal or metal oxide nanoparticles, to enhance their electrocatalytic activity and selectivity[94]. The unique porous structure of 2D COFs provides a stable and confined environment for these catalytic sites, which prevents aggregation and, thus, improves the overall performance[95]. Additionally, 2D COFs can serve as electrochemically active materials that directly participate in electrochemical reactions. Certain COFs can serve as excellent catalysts for important ORR and OER in fuel cells or metal-air batteries. Unlike conventional catalysts, these COFs exhibit high activity, durability, and improved resistance to contaminants[96,97]. Several researchers are actively investigating different synthesis strategies for the design and fabrication of 2D COFs with enhanced electrocatalytic properties[98,99]. These efforts include the development of new 2D COF structures, investigations into different catalytic sites, and the optimization of the electronic and chemical properties of the frameworks to achieve different products and specific reaction requirements. Among them, the HER[100], OER, ORR[101], and CO_2RR[102], which are the most investigated aspects in the field of electrocatalysis, are actively being investigated. Additionally, research cases and strategies for each type of 2D COF electrocatalyst have been introduced. Scheme 3 illustrates a representative ligand building block that forms a 2D COF.

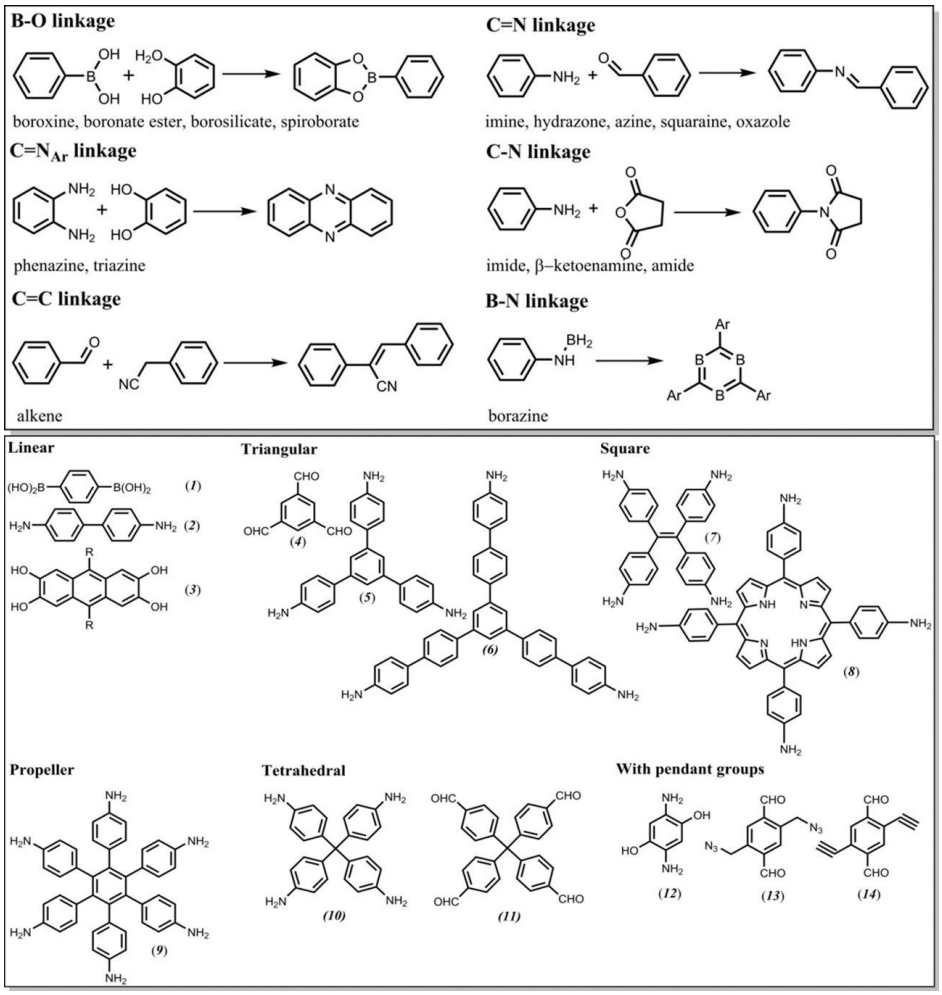

Scheme 3. Typical building block types comprising 2D COFs. Reproduced with permission. Copyright 2018, John Wiley and Sons[103].

HER

Recently, hydrogen has received considerable attention as an alternative energy source to conventional fossil fuels[104]. Research pertaining to hydrogen storage and production using various methods is currently being conducted. In particular, a method for generating hydrogen by decomposing water via an electrochemical method is receiving attention because it requires a precursor other than water; this is referred to as the HER[105]. Rare or transition metals (Pt, Pd, Ru, Co, *etc.*) or ceramics (NiO, Co_2O_3, transition metal dichalcogenide, *etc.*) are the most typically investigated electrocatalytic materials for water splitting[106]. However, these materials are not chemically stable under basic or acidic conditions and are expensive. By contrast, 2D COFs via irreversible reactions are suitable as HER catalysts because they are inexpensive and chemically stable. Metal-free catalysts can be manufactured using only 2D COFs. However, the simultaneous use of 2D COFs and metals to improve electrical conductivity has been reported as well.

Metal-free 2D COF for HER

First, a metal-free 2D COF was introduced [Figure 7A]. Bhunia *et al.* prepared a metal-free 2D COF using two monomers[107]. In particular, 1,3,6,8-tetrakis(4-formylphenyl) pyrene (0.1 mmol, 61 mg) and 5,10,15,20-Tetrakis(4-aminophenyl) porphyrin (0.1 mmol, 67 mg) were added to dimethylacetamide/*o*-dichlorobenzene(*o*-DCB) (3.0/1.0 mL) and sonicated. Subsequently, SB-PORPy-COF was fabricated via heat

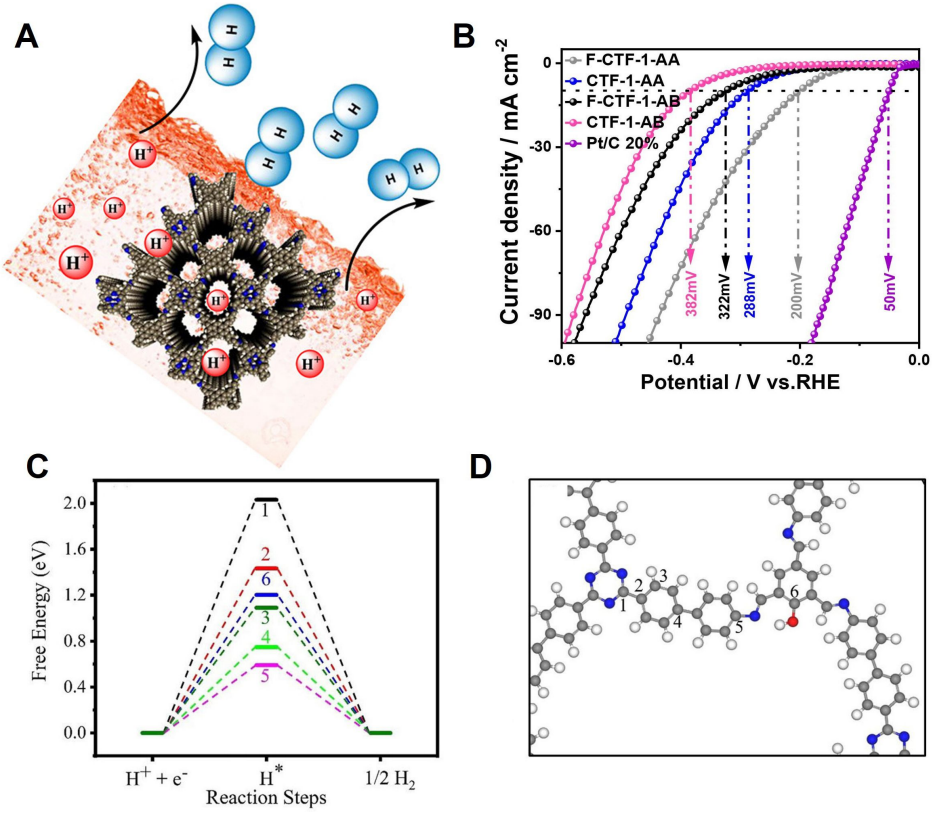

Figure 7. (A) Schematic illustration of 2D COF HER catalyst. Copyright 2017, American Chemical Society[107]. (B) Electrochemical measurement of LSV of CTFs in 0.5 mol L-1 H_2SO_4. Copyright 2023, Elsevier[108]. (C) Free energy plots of HER on unique sites. (D) Model structure showing selected sites for H-atom adsorption. Gray, blue, red, and white spheres represent carbon, nitrogen, oxygen, and hydrogen, respectively. Copyright 2023, John Wiley and Sons[109].

treatment at 120 °C for 7 to 8 h in a vacuum atmosphere. In other words, SB-PORPy-COF was composed of imine-based pyrene and porphyrin. This was verified through PXRD, which confirmed that the stability in acid and base conditions is very high. Also, it is confirmed that the pore size was uniform owing to N_2 adsorption. The π electronic conjugation was maximized while pyrene and porphyrin formed AA stacking (eclipsed). This conducting channel participates in the HER and enables the synthesis of metal-free catalysts. The Tafel slope of SB-PORPy-COF was 116 mV dec^{-1}, and the onset potential at 5 mA cm^{-2} was 380 mV. Zhao *et al.* fabricated 2D-CTFs using 1,4-phenylenonitrile (DCB 2 mmol, 0.256 g) and CF_3SO_3H (1 mmol, 0.088 mL)[108]. After cooling in liquid nitrogen, heat treatment in vacuum, and finally immersion in liquid nitrogen, an AB-stacked (staggered) CTF (CTF-1-AB) was obtained. If DCTFB is removed and processed, then F-CTF-1-AB, to which fluorine has been added, can be generated. If additional heat treatment is performed, then the AA stacking (eclipsed) of CTF-1-AA and F-CT-1-AA can be achieved. AA and AB stacking was confirmed through XRD analysis; furthermore, the analysis confirmed that the structure was maintained even after treatment with fluorine. Comparing the HER performances of the four CTFs, the overpotential of F-CT-1-AA was 200 mV [Figure 7B], which reflected the best catalytic efficiency (Tefal slope: 97 mV dec^{-1}). This is because a unique-conjugated one-dimensional channel was formed during AA stacking, and the hydrogen evolution efficiency increased because the band gap was reduced by fluorine, and the number of carriers increased. Ruidas *et al.* synthesized an imine-based 2D C_6-TRZ-TFP-COF using a C_3-symmetric triamine and trialdehyde monomer[109]. The 2D C_6-TRZ-TFP-COF exhibited an outstanding HER in the absence of metal atoms. Because various hydrogen adsorption sites were considered in various aspects based on DFT calculations and the results of previous studies, a unique result was

obtained. Notably, a high density of electrons among π bonds is advantageous to the HER. However, when comparing the sites of carbon bonded to oxygen and carbon bonded to nitrogen, the sites bonded to nitrogen (electron-deficient) indicated a lower adsorption barrier [Figure 7C and D]. This is because the adsorption of hydrogen onto an already electron-deficient surface can compensate for stronger bonding. Therefore, based on this mechanism, we hypothesize that hydrogen production is realizable using only inexpensive 2D COFs without metal atoms. Halder *et al.* synthesized a triazine-containing polyimide-based COF (TP-COF) using pyromellitic dianhydride (PMDA), melamine, and dimethylformamide (DMF) as precursors[110]. The synthesis involved a relatively simple one-pot condensation method. The surface area and pore size of TP-COF synthesized in this manner were 312.6 $m^2 g^{-1}$ and 1.8 nm, respectively. The surface area of TP-COF-C700, which was heat-treated in N_2 atmosphere for HER applications, increased to 672.2 $m^2 g^{-1}$. The HER performance of TP-COF-C700 was 94 mV@10 mA cm^{-2}. Additionally, a Faradaic efficiency of 98% was maintained for 60 h.

Metal-decorated 2D COF for HER

Next, a catalyst prepared by combining a metal with a 2D COF is introduced. Zhao *et al.* manufactured a hybrid of Ru particles, reduced graphene oxide (rGO), and a 2D COF to increase the electrical conductivity and improve the HER [Figure 8A][111]. A 2D COF was synthesized by mixing piperazine, cyanuric chloride, and potassium carbonate in 1,4-dioxane, followed by performing reflux at 110 °C for 2D. Ru and rGO were synthesized using the 2D COF and refluxing. During the complexation of Ru, Ru ions were formed in the COF nanosheet in particle form, and uniformly distributed Ru particles were achieved without separate dispersion. The formed Ru particles measured 2-2.4 nm, and the results of TEM analysis confirmed that they were uniformly distributed in the nanosheet. The COF/rGO-Ru indicated an overpotential of 42 mV and a low Tefal slope of 46 mV dec^{-1}, which were significantly better than those of commercially available Pt/C [Figure 8B]. However, they were lower compared with those of other Ru-based catalysts. Maiti *et al.* improved the HER by encapsulating Ru in a 2D COF, which was synthesized using 3,4-diaminobenzohydrazide and benzene-1,3,5,-tricarboxaldehyde[112]. The Ru encapsulation was dried after stirring the synthesized 2D COF in a $RuCl_3$ solution. Even after Ru encapsulation, the result of XRD analysis confirmed that no structural change occurred in the 2D COF. In addition, the result of energy dispersive X-ray spectroscopy analysis confirmed that Ru was uniformly distributed on the 2D COF surface. As shown in Figure 8C-E, 2D COFs and $RuCl_3$ were used as comparison groups to evaluate the HER. The resistance value of Ru@COF was extremely low compared with those of the other two groups. In addition, its overpotential improved significantly to 212 mW. This performance was stable as no significant deterioration was indicated even after 100 repetitions of the experiment. Additionally, Ru@COF can be used to conduct electrochemical catalytic experiments without a solid binder. Pan *et al.* synthesized Cryst-2D-PMPI-Ru, which is a combination of 2D COFs and Ru clusters[113]. First, a dianhydride monomer was placed in a round-bottom flask containing a DMF solution and dissolved until it became transparent. Subsequently, melamine was added progressively, and heat was treated for 72 h in a hydrothermal synthesis atmosphere at 180 °C. The prepared 2D COF nanosheet was soaked in $RuCl_3 \cdot xH_2O$. The solution was sonicated for 12 h and thermally decomposed to form Ru clusters on the 2D COF nanosheet [Figure 8F]. At this time, the HER varied with the pyrolysis temperature. During pyrolysis at 800 °C, the ratio of Ru metal (Ru^0) was the highest, and the HER was the best. The overpotential and Tafel slope of Cryst-2D-PMPI-Ru-800 were 55.3 mV and 36.5 mV dec^{-1}, respectively, which were significantly higher than those of Pt/C. These experiments provide evidence that the formation and structure significantly affect the catalytic performance. Wang *et al.* elucidated a procedure for the construction of a durable Mo-based HER chainmail catalyst based on the pyrolysis of Mo and Ni-adsorbed 2D COFs[114]. The resulting chainmail catalyst exhibited an in-situ formed Mo_2C-$MoNi_4$ structure nestled within nitrogen-enriched carbon (Mo_2C-$MoNi_4$@NC). This structure demonstrated an exceptional HER and required a low overpotential of 104 mV. More importantly, the durability was maintained after chronopotentiometry testing for 140,000 s in both acidic and alkaline

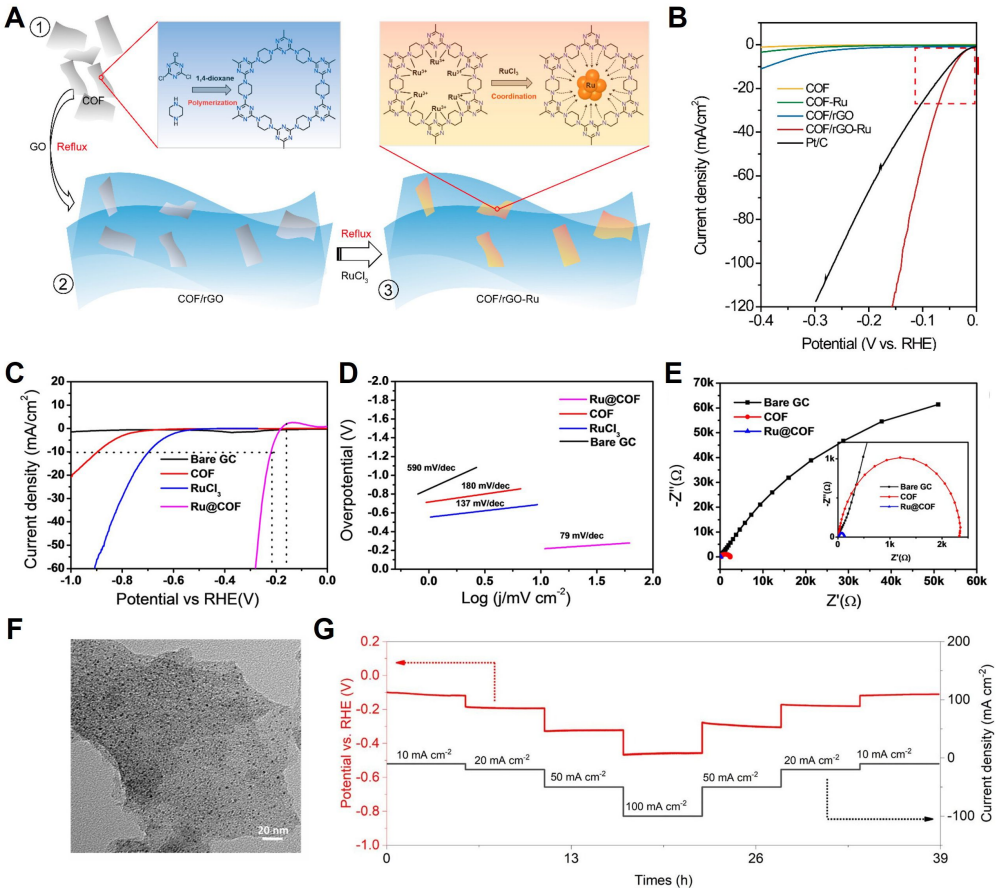

Figure 8. (A) Preparation procedure of COF/rGO-Ru, (B) LSV curves of COF, COF/rGO, COF-Ru, COF/rGO-Ru, and commercial Pt/C. Copyright 2019, American Chemical Society[111]. (C) LSV plot of Ru@COF, bare $RuCl_3$, and COF. (D) Tafel plot of Ru@COF, COF, $RuCl_3$, and bare GC. (E) Nyquist plot of impedance spectra of bare GC, COF, and Ru@COF at onset overpotential of 159 mV. Inset: impedance spectra in a lower frequency range. Copyright 2020, John Wiley and Sons[112]. TEM images of (F) Cryst-2D-PMPI. Copyright 2023 ELSEVIER. Copyright 2021, ELSEVIER[113]. (G) Longtime stability of Mo_2C-$MoNi_4$@NC-2 at current densities of 10, 20, 50, 100, 50, 20, and 10 mA cm^{-2} (each step was set as 20,000 s). Copyright 2023, Elsevier[114].

media, owing to the protective effect of the N-doped graphene shell layer [Figure 8G]. This study offers new perspectives for the development of stable catalysts without noble metals for diverse energy conversion applications.

OER/ORR

Oxygen-related catalysts are a class of materials that contribute significantly to various chemical reactions involving oxygen, such as the ORR[115,116], OER[117-120], and oxygen-based fuel production[121]. These catalysts are designed to facilitate the conversion of oxygen molecules into different chemical species, thus contributing to applications such as fuel cells, metal-air batteries, water splitting, and CO_2 reduction[122]. Oxygen-based catalysts can be based on transition metals, metal oxides, perovskites, or organic materials, and their development aims to improve the reaction kinetics, enhance catalytic activity, and achieve high selectivity and durability, thus ultimately advancing the field of energy conversion and storage[123,124]. Additionally, 2D COFs exhibit unique properties, including large surface areas, ultrahigh porosity, tunable pore sizes, relatively high chemical/thermal stability, and a tailorable architecture. These properties make 2D COFs an attractive material for electrocatalytic reactions such as ORR in fuel cells and OER in electrolytic water splitting and metal-air batteries.

OER

Among the methods for synthesizing free-standing COFs, polymerization occurs at the interface of two solutions[125]. However, implementing this method over a large area is challenging because the diffusion of monomers at the interface is relatively slow. Hence, Tang *et al.* synthesized a 32-nm-thick free-standing Co-porphyrin-based film (CoP-TOB) via polymerization at the interface between air and DMSO [Figure 9A][59]. As shown in Figure 9B, the area of this film was 3,000 cm^2 (50 cm × 60 cm), and it exhibited excellent mechanical stability. Unlike the result of existing methods, hydrolytic stability was achieved owing to the combined use of mesobenzohydrazide and aldehydes. To measure the catalytic performance, glassy carbon was coated with free-standing CoP-TOB. As shown in Figure 9C, the overpotential and Tafel slope of CoP-TOB were 450 mV and 89 mV dec^{-1}, respectively. In addition, its performance in an ORR and all-solid-state Zn-air battery was confirmed, thus demonstrating that it can be used in various applications. By implementing an all-solid-state battery, charging and discharging can be achieved even in the bending state. Yan *et al.* fabricated ultrathin COF nanosheets with a thickness of 1.2 nm using cage-like bicyclocalix[2]arene[2]triazines tri-aldehyde (BCTAL)[126]. Based on DFT calculations, the π-π stacking interaction energy of Cage-COF-1 was approximately 1/50 that of graphite. Therefore, ultrathin COFs were successfully exfoliated via a simple sonication process. The area of the exfoliated nanosheet was 1 to 10 μm [Figure 9D]. Compared with existing processes, this process is advantageous to mass production. The exfoliated ultrathin COF nanosheets were mixed with $Co(CH_3COO)_2{\cdot}4H_2O$ in a CH_2Cl_2/CH_3OH (10:1) solution and treated with Co (Cage-COFs-1Ns/Co). To evaluate the OER, carbon black and Cage-COFs-1Ns/Co were mixed in a Nafion solution, ultrasonicated, and deposited onto glassy carbon to fabricate an electrode. The overpotential and Tafel slope of Cage-COFs-1Ns/Co were 330 mV and 56 mV dec^{-1}, respectively [Figure 9E]. This performance was maintained even after 2,000 iterations [Figure 9F]. Yang *et al.* synthesized 2D-COF-C_4N via a solvothermal reaction between triphenylenehexamine and HKH, and the exact adsorption sites were determined via DFT calculations[127]. First, the valence band maximum and conduction band minimum of 2D-COF-C_4N were confirmed to be the C and N atom sites, respectively. For the OER, the initial step involves the formation of the holes and the subsequent adsorption of H_2O or OH^- on the catalyst surface. Therefore, H_2O or OH^- was adsorbed to the C atom site, and among them, the C_4 site was the most active for adsorption. The overpotential of the 2D-COF-C^4N is 349 mV and the Tafel slope was 64 mV dec^{-1}, thus suggesting an effective strategy for fabricating metal-free catalysts. Composites with various mixed materials were also used for the OER. Cui *et al.* fabricated CoCu-ZIF@GDY using graphdiyne (GDY) nanowires and a CoCu-based zeolitic imidazolate framework nanosheet (CoCu-ZIF-NSs)[128]. CoCu-ZIF@GDY contributed significantly to the electrochemical catalytic reaction because of its high surface area and the mixed state of Co^{2+}/Co^{3+} and Cu^{2+}/Cu^+ ions. In addition, results confirmed that the numerous C atom sites and the highly conjugated structure of GDY improved the OER. In this study, a cell that simultaneously enabled the HER and OER using CoCu-ZIF@GDY as a dual-electrode was used. The HER achieved was better than that yielded by Pt/C/RuO_2. The OER overpotential and Tafel slope of CoCu-ZIF@GDY were approximately 250 mV and 57 mV dec^{-1}, respectively [Figure 9G and H]. In addition, its OER (as shown in Figure 9I) was better than that of IrO_2. Zhang *et al.* proposed an optimal transition metal for producing single-atom catalysts (SAC) with COFs. DFT calculations were performed in this study[129]. These calculations suggested that the transition metals bind to the N site, Ni, and Co, lowering the Gibbs energy barrier for the OER. This is due to strong d-pπ coupling and high charge transfer ability. Subsequently, TM-COF-C_4N was manufactured using Ni, Co, Fe, Mn, and Cu, and it was confirmed that the current densities of Ni and Co were high. As for OER performance, Co-COF-C_4N is 280 mV at 10 mA cm^{-2}, 69 mV. In this study, we predicted the behavior of metal atoms using DFT, followed by experiments to support this. Therefore, this was considered desirable.

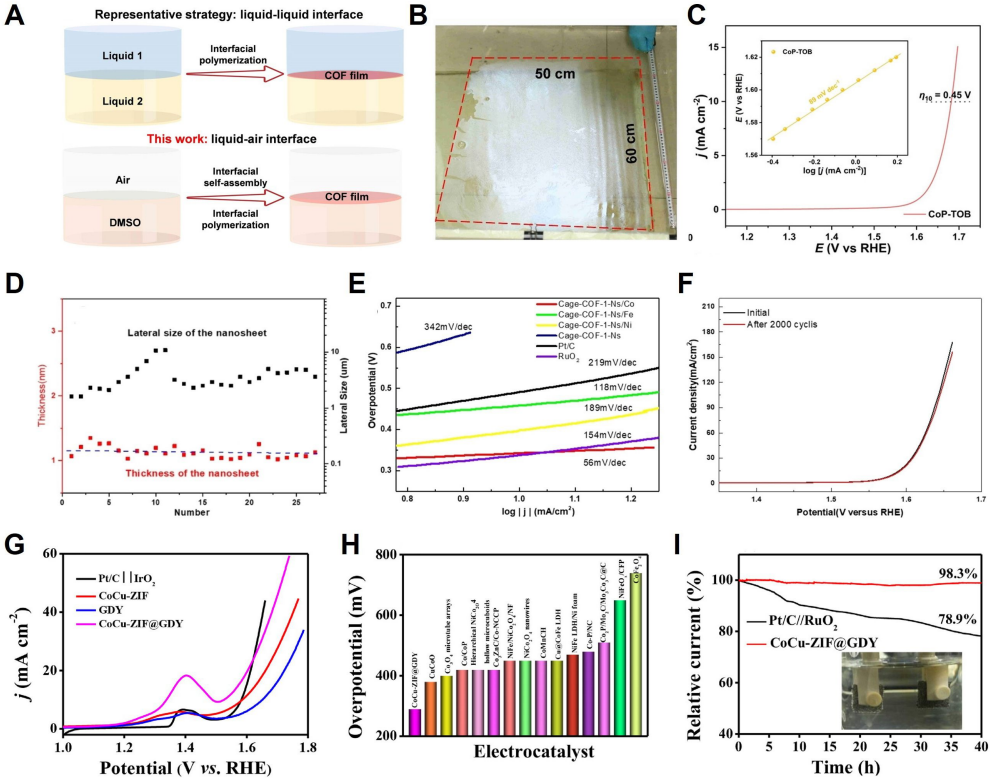

Figure 9. (A) Synthesis of COF films at liquid–liquid and liquid–air interfaces. (B) Photograph of CoP-TOB film floating on water. (C) OER LSV and Tafel slope of CoP-TOB. Copyright 2023, John Wiley and Sons[59]. (D) Thickness and lateral size distribution of exfoliated Cage-COF-1-Ns (horizontal dotted black line indicates the theoretical thickness of a single-layered Cage-COF-1 nanosheet). (E) Tafel slopes of Cage-COF-1-Ns samples in OER. (F) OER polarization curves of Cage-COF-1-Ns/Co before and after 2000 potential cycles. Copyright 2022, John Wiley and Sons[126]. (G) Polarization curves of CoCu-ZIF, GDY, and CoCu-ZIF@GDY in two-electrode electrolyzers based on scan rate of 10 mV s^{-1}; (H) Comparison with reported catalysts under overpotential of 10 mA cm^{-2} in two-electrode electrolyzers; (I) Long-term durability test of CoCu-ZIF@GDY electrolyzers at 10 mA cm^{-2} and photograph showing water splitting (the inset). Copyright 2020, Elsevier[128].

ORR

Fabricating a metal-free catalyst via pyrolysis is inexpensive and useful; however, this technique does not allow the atomic position or structure of COFs to be controlled easily. Martínez-Fernández *et al.* fabricated an ORR catalyst by preparing a metal-free, non-pyrolyzed material[130]. Using this fabrication method, the structure of the link center of XDI$_{0.19}$-CPF (X = N, Bz, and P), which is a diimide-based material, was formed by classifying it into three types, and the differences were confirmed through rigorous analysis [Figure 10A]. This fabrication method is referred to as the click post-synthesis methodology. The bulk material prepared via this method was used to evaluate the performance of the electrochemical catalyst. Among the three types of yielded COFs, BzDI$_{0.17}$-COF was the most suitable material because of the formation of a four-electron pathway under an applied voltage of 0.77 V. The Tafel slope of BzDI$_{0.17}$-COF was -79.9 mV dec^{-1} [Figure 10B and C]. The click post-synthesis methodology presented herein provides effective guidelines for catalyst design. Chang *et al.* fabricated a 2D COF that exhibited two unique properties. Cyclotriphosphazene-based COFs contain abundant C-atom active sites because of their highly electrophilic structure[131]. In addition, the active sites of C atoms are well exposed by the bilayer stacking of the [6+3] imine-linked backbone, and mass diffusion occurs between catalytic reactions. In addition to these two properties, thin COF nanosheets can be fabricated relatively easily via weak interlayer π-π interactions. The π-π interaction energy can be determined by the interlayer spacing, and 14.0 Å was determined to be the appropriate spacing. JUC-610-CON fabricated via this process featured a thickness of 4 nm and a length of 800 nm and can be peeled off [Figure 10D-F]. The Tafel slope of the OER was 61.5 mV dec^{-1}. In addition,

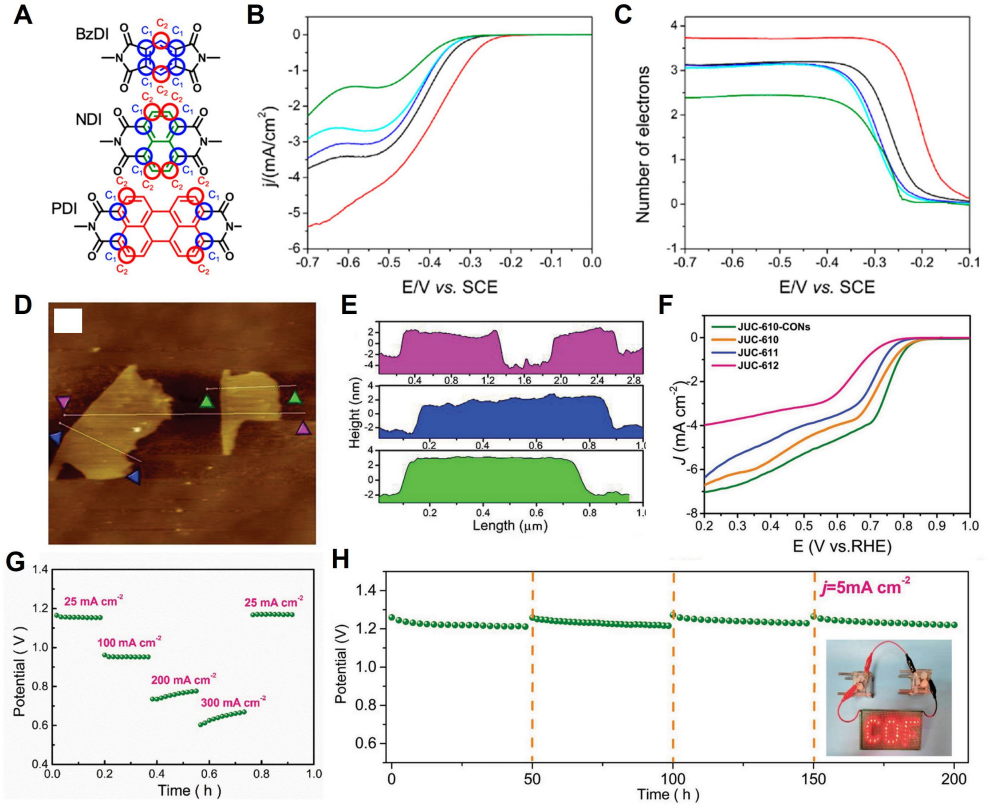

Figure 10. (A) Active ORR sites detected within NDI, BzDI, and PDI moieties via DFT calculations and denoted as C_1 (blue circles) and C_2 (red circles). (B) Hydrodynamic linear sweep voltammetry and (C) number of electrons exchanged in ORR at different potentials using RRDE of GC/Pt (disc/ring) modified with $BzDI_{0.17}$-COF/Carbon SuperP (black), $NDI_{0.17}$-COF/Carbon SuperP (red), PDI0.17-COF/Carbon SuperP (blue), TAPB-DMTA-COF/Carbon SuperP (cyan), and Carbon Super P (green) in O_2 saturated 0.1 M NaOH solution at 10 mV/s and 1,000 rpm. Copyright 2023, American Chemical Society[130]. (D) AFM image of JUC-610-CON, and (E) the corresponding height curves for selected areas in (D). (F) LSV curves of JUC-610-CON, JUC-610, JUC-611, and JUC-612 at 1,600 rpm in O^{2-} saturated 0.1 M KOH electrolyte. (G) Discharge curves of JUC-610-CON-based ZAB at different current densities (25, 100, 200, and 300 mA cm^{-2}). (H) Stability of JUC-610-CON-based ZAB at 5 mA cm^{-2} in ambient air conditions, and photographs of red "COF" LED panel powered by two ZABs in series (inset). Copyright 2023, Springer Nature[131].

the JUC-610-CON as a Zn-air battery demonstrated a delivered power density of 156 mW cm^{-2} at 300 mA cm^{-2} [Figure 10G and H]. When using a 2D COF as a catalyst, its crystallinity and porosity are particularly important. García-Arroyo *et al.* showed that 2D COFs exhibited different ORRs depending on their crystallinity and porosity[132]. A DAPT-TFP-COF was realized by synthesizing 2,7-diaminopyrene-4,5,9,10-tetraone (DAPT) and 2,4,6-TFP under solvothermal conditions. For comparison, an amorphous DAPT-TFP-polymer with a chemical composition similar to that of DAPT-TFP-NA was prepared. The LSV curve confirmed that the DAPT-TFP-COF with the highest crystallinity and porosity exhibited the highest current density. DFT calculations were performed to confirm the ORR active sites. The results show that O_2 adsorption occurred the most in the beta-carbon site. Additionally, the experimental results showed that COFs synthesized without metal or additional carbon treatment can be used as ORR catalysts, depending on their crystallinity and porosity. Kumar *et al.* successfully synthesized a Fe-phthalocyanine-derived highly conjugated 2D COF (2D FePc-COF) using a microwave reactor after mixing 1 mol cyclohexanone and 3 mol OA-FePc with xylene and ethanol[133]. At this time, the microwave reactor condition is 300 W and 120 °C. In this study, 2D FePc-COF outperformed 20% Pt/C in ORR performance. In addition, stability was confirmed via 10,000 CV tests. The mechanism underlying this performance is elucidated by DFT calculations. The extended conjugation and removal of the electron donating group ($-NH_2$) were found to shift the energy of the d_z2 orbital (Fe) closer to the π^* orbital (O_2), resulting in the optimal coupling of the

two orbitals. This was subsequently confirmed. In other words, they predict that the extended junction of 2D FePc-COF will reduce the d_z2(Fe) orbital energy and move it closer to the π^* orbital (O_2), improving interorbital coupling and leading to a 4e$^-$ORR with lower overpotentials. Furthermore, 2D FePc-COF exhibited a low Tafel value of 80 mV dec^{-1}.

CO_2RR

Because CO_2 is one of the most significant contributors to global warming, technology for reducing CO_2 using various methods has been continuously developed[102,134-138]. Recently, the utilization of CO_2RR beyond storage has received significant attention[139-141]. Unlike previous types of electrocatalysts for the CO_2RR, metallic materials are particularly advantageous. Among them, Cu is well known for its ability to generate various products via the CO_2RR[142]. However, increasing and controlling product selectivity is difficult. In addition, various metal atoms, such as Ni, Co, and Pd, are alloyed and used in a few cases; however, identifying the CO_2RR site is difficult, which renders it challenging to secure stability. Single-atom catalysis has been extensively investigated as an alternative to metallic materials; however, achieving single-atom control is difficult. Therefore, 2D COF CO_2RR catalysts should be developed to be less dependent on metal elements compared to the catalysts composed of alloys or single metal atoms. In general, because the electrical conductivity of 2D COFs is low, it can be improved using various methods. CO_2RR catalysts can be synthesized using 2D COFs containing donor-acceptor heterojunctions (D-A heterojunctions). Wu *et al.* developed a 2D cobalt porphyrin-based COF (TT-Por(Co)-COF) via the Schiff base reaction of thieno[3,2-b]thiophene-2,5-dicarbaldehyde (TT) containing an electron donor and Co-TAPP containing an acceptor[143]. The electrical properties of the prepared catalysts were improved by D-A heterojunctions. The electrical conductivity was 1.38 × 10^{-8} S m^{-1}, and the carrier mobility was 0.18 cm^2 V^{-1} s^{-1}. In terms of the CO_2 RR performance of TT-Por(Co)-COF, the Faraday efficiency of CO (FE_{CO}) was 91.4% at -0.6 V, and an extremely high current density of 7.28 mA cm^2 was indicated at -0.7 V [Figure 11A, B and C]. Using a similar strategy, Zhu *et al.* fabricated highly crystalline metalloporphyrin-TTF-based COFs (M-TTCOFs) by assembling metallized 5,10,15,20-tetrakis (4-aminophenyl) porphinato (MTAPP, M = Co or Ni) and 2,3,6,7-tetra (4-formylphenyl)tetrathiafulvalene (4-formyl-TTF)[144]. In this regard, TTF served as an electron donor, and an electron path was constructed using metalloporphyrin. DFT calculations confirmed that these electron donors and paths provided more favorable The unit of mobility is in this format.conditions for *COOH and *CO production by providing abundant electrons to the Co atom sites [Figure 11D and E]. The FE_{CO} at -0.7 V of the Co-TTCOF nanosheet prepared as such was 91.3%, which remained stable even after a reaction time exceeding 40 h. The maximum FE_{CO} was 99.7% at -0.8 V [Figure 11F and G].

The second strategy involves the addition of metal atoms and conductive materials. Lu *et al.* improved the CO_2RR by adding Co-porphyrin and amino-functionalized carbon nanotubes (CNTs) to a synthesized COF[145]. The 2D COF was synthesized using TAPP. To add Co atoms, TAPP and $Co(CH_3COO)_2{\cdot}4H_2O$ were added to a DMF solution, and reflux was performed. Subsequently, Co-TAPP, terephthalaldehyde, and the dispersion of CNTs were placed in ethanol, followed by sonication; finally, COF-366-Co@CNT was achieved by degassing in liquid nitrogen. A catalyst with an excellent CO_2RR was achieved owing to the strong binding force between the CNT and TAPP. COF-366-Co@CNT indicated a FE_{CO} of 93.6% at -0.68 V [Figure 12A]. Subsequently, Zhang *et al.* synthesized a 2D conductive Ni-phthalocyanine-based COF (NiPc-COF) using 2,3,9,10,16,17,23,24-octaaminophthalocyanato Ni(II) and tert-butylpyrene-tetraone[146]. NiPc-COF confirmed that Ni ions were evenly distributed through TEM analysis, and the area and thickness of the nanosheet were 3 μm and 0.74 nm, respectively, based on AFM measurement. The CO_2RR indicated a FE_{CO} exceeding 93% over a wide voltage range of -0.6 to -1.1 V. In particular, at -0.9 V, it was approximately 100% [Figure 12B and C]. In addition, the CO generation efficiency was maintained even after 10 h of catalytic reaction. CO_2 was adsorbed on the Ni center as COOH*, converted to CO, and desorbed again. This study presents an effective strategy for electrocatalysis using a 2D COF nanosheet. Meanwhile,

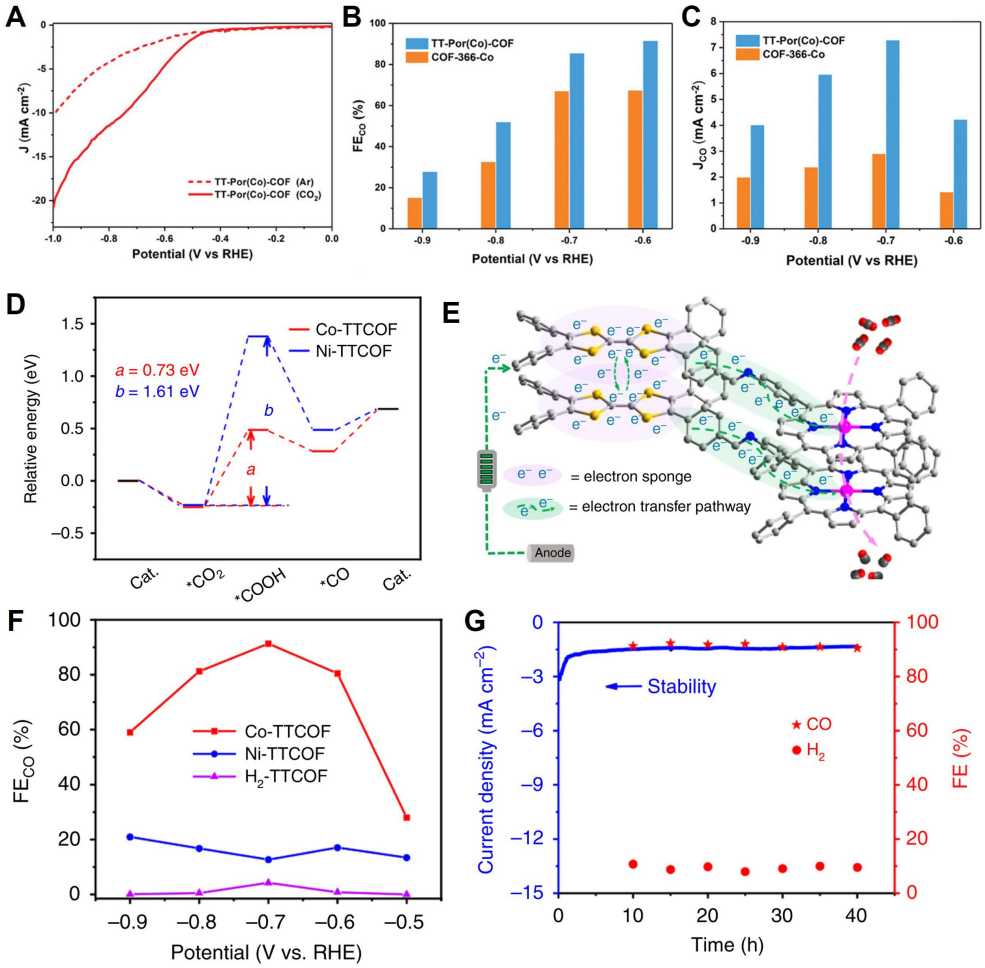

Figure 11. (A) LSV curves in CO_2-saturated and Ar-saturated 0.5 m $KHCO_3$ under scan rate of 10 mV s^{-1}. (B) FE_{CO} and (C) J_{co} from -0.6 to -0.9 V *vs.* RHE of TT-Por(Co)-COF and COF-366-Co. Copyright 2020, John Wiley and Sons[143]. (D) Relative energy diagrams of CO_2 reduction to CO for M-TTCOFs (M = Co or Ni). (E) Proposed schematic mechanism for electrocatalytic CO_2RR on Co-TTCOF. (F) FE_{CO} based on a calculated overpotential range from -0.5 to -0.9 V. (G) Cycling stability test of Co-TTCOF at potential of -0.7 V *vs.* RHE. Copyright 2020, Springer Nature[144].

sacrificial materials were used to control active sites in previous studies. After synthesizing Co-COF on hydrotalcite, Miao *et al.* increased the number of CoN_2O_2 sites via heat and acid treatment[147]. Hydrotalcite has a hexagonal base crystal structure, and the Co-COF grown on it exhibits a regular mesoporous structure, depending on the crystallinity of the substrate [Figure 12D]. In the pyrolysis process, the substrate assumes two roles. First, Co-ion aggregation is prevented, and CoN_2O_2 formation is advantageous because of the sufficient oxygen supply. DFT calculations confirmed that CoN_2O_2 exhibited the lowest COOH* adsorption energy barrier compared with any other sites. In addition, the binding of COOH* to CoN_2O_2 was promoted because the 2p orbital of COOH* overlapped with the t2g orbital of CoN_2O_2 [Figure 12E and F]. The FE_{CO} of 2D-Co-COF500 prepared as such was approximately 50% at -0.7 and -0.8 V. Catalysts using metal particles exhibit stability problems such as oxidation and agglomeration. Zhang *et al.* produced a Cu-cluster/COF structure by reducing a COF containing Cu atoms[137]. Sonication was performed by mixing 2,3,9,10,16,17,23,24-octahydroxyphthalocyaninato copper (CuPc-8OH, 95+%), Tetrafluorophthalonitrile (99%, TFPN), and N,N-Dimethylacetamide (DMA, AR). Subsequently, freeze-drying was performed in a liquid nitrogen atmosphere at 77 K. The material thus produced was heat treated at 150 °C for 120 h, washed with MA, DMF, H_2O, CH_2Cl_2, and THF, and dried. In the Cu Cluster generation process, the synthesized COF was dispersed in water and sonicated by adding 2M $Cu(ClO_4)_2{\cdot}6H_2O$ solution.

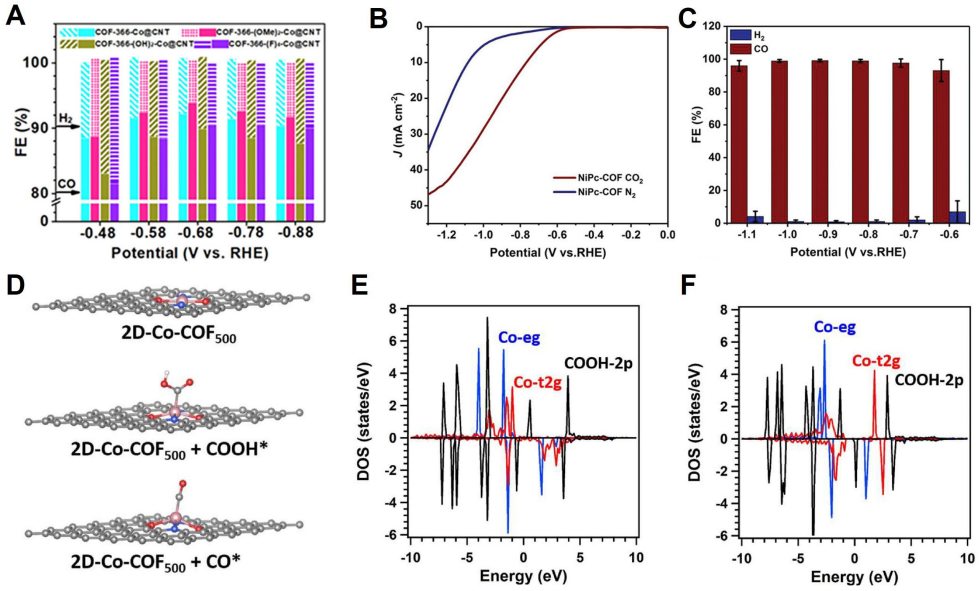

Figure 12. (A) FEs of COF-366-Co@CNT, COF-366-$(OMe)_2$-Co@CNT, COF-366-$(OH)_2$-Co@CNT, and COF-366-$(F)_4$-Co@CNT at a scan rate of 5 mV s^{-1}. Copyright 2020, American Chemical Society[145]. (B) LSV curves of NiPc-COF in CO_2-saturated and N_2-saturated 0.5 m $KHCO_3$ electrolytes at a scan rate of 10 mV S^{-1}. (C) FE_{CO} and FEH_2 from -0.6 to -1.1 V of NiPc-COF in CO_2-saturated 0.5 m $KHCO_3$ electrolytes. Copyright 2020, John Wiley and Sons[146]. (D) Proposed schematic mechanism for electrocatalytic CO_2RR on 2D-Co-COF_{500}. (E) PDOS before COOH adsorbed on 2D-Co-COF_{500}. (F) PDOS before COOH adsorbed on Co-COF_{500}. Copyright, 2022 Elsevier[147].

For the reduction reaction, Cu nanocluster (NC)@CuPc-COF was prepared by heat treatment in an Ar atmosphere. The Cu clusters produced in this manner exhibit very high stability owing to the confinement effect of the COF. The Cu clusters embedded in the COF were confirmed by TEM analysis of these structures. In this study, CH_4 was used as the target product, and it exhibited a faraday efficiency of ~74 ± 3%. Although it is not a metal-free COF, it can be used as an auxiliary catalyst for various products. In Table 1, various 2D COF catalysts used in diverse energy conversion applications are summarized, along with the key factors relevant to their respective uses.

CONCLUSION AND OUTLOOK

These 2D COFs have yielded promising results. However, their development is still in the early stages, and their practical application in industry is not foreseeable in the near future. A comprehensive analysis of the studies introduced earlier reveals that whether they are metal-free or support metal-based catalysts, COF catalysts are highly chemically stable. The advantage allows for applications across a wide range of pH conditions and oxidizing or reducing environments, presenting clear opportunities for various industrial uses. Nevertheless, while 2D COFs show promise, their immediate applications in the industry remain uncertain. In a recent study, the number of electrochemical catalyst sites was compared and analyzed according to the COF dimensions (1D, 2D, and 3D)[148]. The biggest problem with 2D COFs is that they lack catalytically active sites when compared to 1D COFs. Additionally, numerous problems remain, such as performance competitiveness with metal catalysts and sustainability of productivity. To fully exploit the potential of 2D COF catalysts, a wide range of materials should be developed and their placement optimized. Additionally, 2D COF materials offer several advantages, such as low cost, high stability in acidic or basic environments, and specialized mass transport through crystallinity or porosity. Furthermore, their usability is enhanced by their ability to predict catalytic effects and sites through precursor selection and framework design. Whereas the efficiency of small-scale catalysts may be limited, they are expected to contribute significantly to large-scale industrial production lines for reactions such as the HER, OER, ORR, and CO_2RR. To exploit these advantages, the following developments must be addressed.

Table 1. Various electrocatalysts using 2D COFs

The type of catalysis	COF	BET surface area ($m^2 g^{-1}$)	Electrolyte	Tafel slope ($mV dec^{-1}$)	Overpotential (mV)	Faradaic efficiency (%)	Product	Reference
HER	SB-PORPy-COF	869	0.5 M H_2SO_4	116				[107]
	F-CT-1-AA	741		97	200			[108]
	2D C_6-TRZ-TFP-COF	928	0.5 M H_2SO_4	82	200			[109]
	COF/rGO		1.0 M KOH	46	42			[111]
	Ru@COF		1.5 M H_2SO_4	79	212			[112]
	Cryst-2D-PMPI-Ru		0.5 M H_2SO_4 1.0 M KOH	36.5	55.3			[113]
	Mo_2C-$MoNi_4$@NC-2	108.7	0.5 M H_2SO_4	93	104			[114]
	TP-COF-C700	672.2	1.0 M KOH	128	94			[110]
OER	CoP-TOB		0.1 M KOH	89	450			[59]
	2D COF Cage-COF-1-Ns/Co		1 M KOH	56	330			[126]
	2D-COF-C_4N		1 M KOH	64	349			[127]
	CoCu-ZIF@GDY		0.1 M KOH	57	250			[128]
	Co-COF-C_4N		0.5 M Na_2SO_4	43	280			[129]
ORR	$NDI_{0.17}$-CPF	158	0.1 M NaOH	79.9				[130]
	Q3CTP-COFs (JUC-610-CON)	475	0.1 M KOH	61.95				[131]
	DAPT-TFP-COF	200	0.1 M NaOH					[132]
	2D FePc-COF		0.1 M KOH	80				[133]
CO_2RR	TT-Por(Co)-COF	748	0.5 M $KHCO_3$			91.4 (-0.6 V)	CO	[143]
	TTF-based COFs (Co-TTCOFs)		0.5 M $KHCO_3$	237		99.7 (-0.8 V)	CO	[144]
	COF-366-$(OMe)_2$-Co@CNT	196	0.5 M $KHCO_3$	190		93.6 (-0.68 V)	CO	[145]
	Ni-phthalocyanine-based COF (NiPc-COF)	358	0.5 M $KHCO_3$			~100 (-0.9 V)	CO	[146]
	2D-Co-COF_{500}	123	0.5 M $KHCO_3$			96.5 (-0.8 V)	CO	[147]
	Cu-NC@CuPc-COF		1 M KOH			74.3 (-1.0 V)	CH_4	[148]

Enhancing Performance: Currently, pure 2D COFs perform worse than catalysts composed of bulky metal or single metal atoms. Increasing the current density during catalytic reactions is essential. This can be achieved by increasing the number of catalytic sites or improving the electrical conductivity. However, matching the performances of metal-based catalysts is challenging. Therefore, extensive research is required to investigate the use of other materials and heterostructures that can serve as cocatalysts or facilitate material transport to maximize the surface area. Strategies aimed at maximizing these roles must be continuously pursued.

Improving Synthesis Methods: The synthesis of 2D COF materials is generally time-consuming and can hinder productivity, even when inexpensive materials are used. These aspects are major disadvantages to price competitiveness. As most 2D COFs use organic precursors, low process temperatures are typically required, rendering mass synthesis and production unfavorable owing to the slow decomposition, diffusion, and rebonding of the precursors. The low speed and yield of the synthesized materials pose significant challenges. Hence, appropriate techniques must be developed to enable the rapid synthesis of large quantities of 2D COFs. One potential solution is to synthesize a 2D COF directly on an electrode to eliminate the additional binding steps. The development of binder-free catalysts can result in higher yields. However, the biggest obstacle to the industrial application of the current catalysts is the manufacturing of large-area electrodes. Given that the process temperature of COF is relatively low, it is expected to be advantageous for manufacturing large-area electrodes. This implies that the development of mass and large-area production is essential to gain industrial merit in the field of 2D COF catalyst usage.

Identifying Active Sites: Determining the active sites in catalyst materials is crucial; however, it involves predicting atomic-level interactions that are complex and require extreme caution. Although DFT calculations are typically performed, they should be applied early in the design stage of catalytic materials instead of solely to confirm active sites. Designing a new 2D COF involves predicting the site and optimizing the performance through continued cross-validation, adjustment steps, performance evaluation, and DFT calculations. This approach maximizes the advantages of 2D COFs by enabling the synthesis of various structures and components.

Expanding CO_2RR Catalyst Functionality: Research pertaining to CO_2RR catalysts using COFs is currently limited to products primarily involving CO^-. Compared with metal-based catalysts, COF catalysts exhibit inferior functionalities. To achieve various products such as CH_4, C_2H_4, and formic acid, the adsorption of CO is crucial. Designing sites that can adsorb CO is challenging as the ability of 2D COF materials to adsorb CO is inherently inferior to that of metal atoms because of the favorability of the d-orbital in most adsorption sites. Consequently, the inclusion of transition metal atoms must be considered in studies pertaining to the CO_2RR. The development of optimized catalyst materials that combine metal atoms and 2D COFs is crucial for industrial applications.

Advancing Full-Cell Research: Whereas recent studies pertaining to catalyst materials focus primarily on half-cells, comprehensive investigations into full cells are essential. The current understanding of electrocatalysts is primarily derived from a material science perspective. However, for wider applicability, the electrolyte, CO_2, product transport, and counter electrodes must be optimized.

Stability or recyclability/reusability: 2D COFs hold promises for catalytic applications due to their stability under various chemical and thermal conditions and their potential for recyclability and reusability in

heterogeneous catalysis. However, the success of COFs as catalysts depends on their design to withstand specific reaction conditions, addressing catalyst deactivation issues, and optimizing the practical aspects of recycling and regeneration processes to make them cost-effective and environmentally sustainable. Researchers should explore and develop COF-based catalysts with improved stability and recyclability for a wide range of applications.

Structural design can be classified into three types: completely metal-free, using metal atoms, and supporting a metal catalyst. As mentioned previously, COFs are generally chemically stable. For each COF, its active catalytic site, mechanical properties, and performance are diverse. Therefore, we propose research aimed at improving system efficiency by using cocatalysts that contribute actively rather than merely serving as structural supports for other catalysts. To develop such systems, it is crucial to investigate the effects that arise when these materials are combined with others. For instance, in the earlier mentioned studies, where Cu clusters and 2D COFs were combined, the COF effectively functioned as a catalyst in the reduction reaction. Therefore, it is essential to establish a distinct and active role in catalytic reactions, as opposed to merely serving as a passive support material.

In conclusion, the development of catalysts using 2D COF materials is highly promising. However, several challenges must be addressed to enable practical industrial applications. Enhancing the performance, improving synthesis methods, identifying active sites, expanding electrocatalyst functionality, and advancing full-cell research are key areas that require focused attention to unravel the full potential of 2D COF catalysts in various industrial processes.

DECLARATIONS

Authors' contributions

Proposed the topic of this review: Yu HK, Kim SY
Prepared the manuscript: Cho JH, Kim Y

Availability of data and materials

Not applicable.

Financial support and sponsorship

This research was supported by the National Research Foundation of Korea (NRF), funded by the Korean government (2021R1A4A3027878, 2022M3H4A1A01012712).

Conflicts of interest

All authors declared that there are no conflicts of interest.

Ethical approval and consent to participate

Not applicable.

Consent for publication

Not applicable.

REFERENCES

1. Chu S, Majumdar A. Opportunities and challenges for a sustainable energy future. *Nature* 2012;488:294-303. DOI PubMed
2. Meys R, Kätelhön A, Bachmann M, et al. Achieving net-zero greenhouse gas emission plastics by a circular carbon economy. *Science* 2021;374:71-6. DOI
3. Duan X, Xu J, Wei Z, et al. Metal-free carbon materials for CO_2 electrochemical reduction. *Adv Mater* 2017;29:1701784. DOI
4. Wang J, Dou S, Wang X. Structural tuning of heterogeneous molecular catalysts for electrochemical energy conversion. *Sci Adv* 2021;7:eabf3989. DOI PubMed PMC
5. Habtamu A, Ujihara M. The mechanism of water pollutant photodegradation by mixed and core-shell WO_3/TiO_2 nanocomposites. *RSC Adv* 2023;13:12926-40. DOI PubMed PMC
6. Motora KG, Wu C, Chala TF, Chou M, Kuo CJ, Koinkar P. Highly efficient photocatalytic activity of Ag_3VO_4/$WO_{2.72}$ nanocomposites for the degradation of organic dyes from the ultraviolet to near-infrared regions. *Appl Surf Sci* 2020;512:145618. DOI
7. Motora KG, Wu C. Magnetically separable highly efficient full-spectrum light-driven $WO_{2.72}$/Fe_3O_4 nanocomposites for photocatalytic reduction of carcinogenic chromium (VI) and organic dye degradation. *J Taiwan Inst Chem Eng* 2020;117:123-32. DOI
8. Zhou Y, Sung J, Brutschea E, et al. Bilayer Wigner crystals in a transition metal dichalcogenide heterostructure. *Nature* 2021;595:48-52. DOI
9. Nguyen TV, Nguyen TP, Le QV, Dao DV, Ahn SH, Kim SY. Synthesis of very small molybdenum disulfide nanoflowers for hydrogen evolution reaction. *Appl Surf Sci* 2023;607:154979. DOI
10. Shin H, Eom W, Lee KH, Jeong W, Kang DJ, Han TH. Highly electroconductive and mechanically strong $Ti_3C_2T_x$ MXene fibers using a deformable MXene gel. *ACS Nano* 2021;15:3320-9. DOI
11. Do HH, Tekalgne MA, Le QV, Cho JH, Ahn SH, Kim SY. Hollow Ni/NiO/C composite derived from metal-organic frameworks as a high-efficiency electrocatalyst for the hydrogen evolution reaction. *Nano Converg* 2023;10:6. DOI PubMed PMC
12. Lee MK, Shokouhimehr M, Kim SY, Jang HW. Two-dimensional metal-organic frameworks and covalent-organic frameworks for electrocatalysis: distinct merits by the reduced dimension. *Adv Energy Mater* 2022;12:2003990. DOI
13. Xue Y, Zhang Q, Wang W, Cao H, Yang Q, Fu L. Opening two-dimensional materials for energy conversion and storage: a concept. *Adv Energy Mate* 2017;7:1602684. DOI
14. Mu Q, Zhu W, Li X, et al. Electrostatic charge transfer for boosting the photocatalytic CO_2 reduction on metal centers of 2D MOF/rGO heterostructure. *Appl Catal B* 2020;262:118144. DOI
15. Voiry D, Yang J, Chhowalla M. Recent strategies for improving the catalytic activity of 2D TMD nanosheets toward the hydrogen evolution reaction. *Adv Mater* 2016;28:6197-206. DOI PubMed
16. Côté AP, Benin AI, Ockwig NW, O'Keeffe M, Matzger AJ, Yaghi OM. Porous, crystalline, covalent organic frameworks. *Science* 2005;310:1166-70. DOI PubMed
17. Mohamed Samy M, Mekhemer IM, Mohamed MG, et al. Conjugated microporous polymers incorporating Thiazolo[5,4-d]thiazole moieties for sunlight-driven hydrogen production from water. *Chem Eng J* 2022;446:137158. DOI
18. Dutta S, Bhaumik A, Wu KC. Hierarchically porous carbon derived from polymers and biomass: effect of interconnected pores on energy applications. *Energy Environ Sci* 2014;7:3574-92. DOI
19. Chen J, Tao X, Li C, et al. Synthesis of bipyridine-based covalent organic frameworks for visible-light-driven photocatalytic water oxidation. *Appl Catal B* 2020;262:118271. DOI
20. Contreras-pereda N, Pané S, Puigmartí-luis J, Ruiz-molina D. Conductive properties of triphenylene MOFs and COFs. *Coord Chem Rev* 2022;460:214459. DOI
21. Bian G, Yin J, Zhu J. Recent Advances on conductive 2D covalent organic frameworks. *Small* 2021;17:e2006043. DOI PubMed
22. Shen J, Zhang R, Su Y, et al. Polydopamine-modulated covalent organic framework membranes for molecular separation. *J Mater Chem A* 2019;7:18063-71. DOI
23. Chen L, Wang W, Tian J, et al. Imparting multi-functionality to covalent organic framework nanoparticles by the dual-ligand assistant encapsulation strategy. *Nat Commun* 2021;12:4556. DOI PubMed PMC
24. Spitler EL, Koo BT, Novotney JL, et al. A 2D covalent organic framework with 4.7-nm pores and insight into its interlayer stacking. *J Am Chem Soc* 2011;133:19416-21. DOI
25. Deng JH, Luo J, Mao YL, et al. π-π stacking interactions: non-negligible forces for stabilizing porous supramolecular frameworks. *Sci Adv* 2020;6:eaax9976. DOI PubMed PMC
26. Jati A, Dey K, Nurhuda M, Addicoat MA, Banerjee R, Maji B. Dual metalation in a two-dimensional covalent organic framework for photocatalytic C-N cross-coupling reactions. *J Am Chem Soc* 2022;144:7822-33. DOI
27. Zhang M, Tong Y, Sun Z, et al. Two-dimensional covalent organic framework with synergistic active centers for efficient electrochemical sodium storage. *Chem Mater* 2023;35:4873-81. DOI
28. Khalid NR, Ilyas S, Ali F, et al. Novel Sn-doped WO_3 photocatalyst to degrade the organic pollutants prepared by green synthesis approach. *Electron Mater Lett* 2024;20:85-94. DOI
29. Dalapati S, Addicoat M, Jin S, et al. Rational design of crystalline supermicroporous covalent organic frameworks with triangular topologies. *Nat Commun* 2015;6:7786. DOI PubMed PMC
30. Farha OK, Eryazici I, Jeong NC, et al. Metal-organic framework materials with ultrahigh surface areas: is the sky the limit? *J Am*

Chem Soc 2012;134:15016-21. DOI
31. Rodríguez-San-Miguel D, Montoro C, Zamora F. Covalent organic framework nanosheets: preparation, properties and applications. *Chem Soc Rev* 2020;49:2291-302. DOI
32. Jin F, Wang T, Zheng H, et al. Bottom-up synthesis of covalent organic frameworks with quasi-three-dimensional integrated architecture via interlayer cross-linking. *J Am Chem Soc* 2023;145:6507-15. DOI
33. Abuzeid HR, El-mahdy AF, Kuo S. Covalent organic frameworks: design principles, synthetic strategies, and diverse applications. *Giant* 2021;6:100054. DOI
34. Cai Y, Wen X, Wang Y, et al. Preparation of hyper-crosslinked polymers with hierarchical porous structure from hyperbranched polymers for adsorption of naphthalene and 1-naphthylamine. *Sep Purif Technol* 2021;266:118542. DOI
35. Katekomol P, Roeser J, Bojdys M, Weber J, Thomas A. Covalent triazine frameworks prepared from 1,3,5-tricyanobenzene. *Chem Mater* 2013;25:1542-8. DOI
36. Tian Y, Zhu G. Porous aromatic frameworks (PAFs). *Chem Rev* 2020;120:8934-86. DOI PubMed
37. Saber AF, Sharma SU, Lee J, El-mahdy AF, Kuo S. Carbazole-conjugated microporous polymers from Suzuki-Miyaura coupling for supercapacitors. *Polymer* 2022;254:125070. DOI
38. Park CG, Yang JW, Hwang NM. TEM Observations of metastable nanocarbon allotropes in the initial stage of diamond growth at 300 °C during diamond hot filament CVD. *Electron Mater Lett* 2023;19:316-24. DOI
39. Hao S, Zhang T, Fan S, Jia Z, Yang Y. Preparation of COF-TpPa1 membranes by chemical vapor deposition method for separation of dyes. *Chem Eng J* 2021;421:129750. DOI
40. Zheng W, Tsang C, Lee LYS, Wong K. Two-dimensional metal-organic framework and covalent-organic framework: synthesis and their energy-related applications. *Mater Today Chem* 2019;12:34-60. DOI
41. Liu M, Liu Y, Dong J, et al. Two-dimensional covalent organic framework films prepared on various substrates through vapor induced conversion. *Nat Commun* 2022;13:1411. DOI PubMed PMC
42. Roy N, Kundu T. Photoresponse of CVD grown crystalline quantum dot-embedded covalent organic framework thin film. *RSC Adv* 2023;13:3669-76. DOI PubMed PMC
43. Li Y, Zhang M, Guo X, et al. Growth of high-quality covalent organic framework nanosheets at the interface of two miscible organic solvents. *Nanoscale Horiz* 2018;3:205-12. DOI
44. Shao M, Zhang Q, Wei X, et al. Twisted node modulation of 2D-COFs for programmable long-afterglow luminescence. *Cell Rep Phys Sci* 2023;4:101273. DOI
45. Sick T, Rotter JM, Reuter S, et al. Switching on and off interlayer correlations and porosity in 2D covalent organic frameworks. *J Am Chem Soc* 2019;141:12570-81. DOI
46. Belov AS, Voloshin YZ, Pavlov AA, et al. Solvent-induced encapsulation of cobalt(II) ion by a boron-capped tris-pyrazoloximate. *Inorg Chem* 2020;59:5845-53. DOI
47. Wei H, Chai S, Hu N, Yang Z, Wei L, Wang L. The microwave-assisted solvothermal synthesis of a crystalline two-dimensional covalent organic framework with high CO_2 capacity. *Chem Commun* 2015;51:12178-81. DOI
48. Zhu D, Zhu Y, Yan Q, et al. Pure crystalline covalent organic framework aerogels. *Chem Mater* 2021;33:4216-24. DOI
49. Kang C, Zhang Z, Wee V, et al. Interlayer shifting in two-dimensional covalent organic frameworks. *J Am Chem Soc* 2020;142:12995-3002. DOI
50. Huang W, Jiang Y, Li X, et al. Solvothermal synthesis of microporous, crystalline covalent organic framework nanofibers and their colorimetric nanohybrid structures. *ACS Appl Mater Interfaces* 2013;5:8845-9. DOI
51. Shevate R, Shaffer DL. Large-area 2D covalent organic framework membranes with tunable single-digit nanopores for predictable mass transport. *ACS Nano* 2022;16:2407-18. DOI PubMed
52. Ji W, Hamachi LS, Natraj A, et al. Solvothermal depolymerization and recrystallization of imine-linked two-dimensional covalent organic frameworks. *Chem Sci* 2021;12:16014-22. DOI PubMed PMC
53. Xu L, Ding SY, Liu J, Sun J, Wang W, Zheng QY. Highly crystalline covalent organic frameworks from flexible building blocks. *Chem Commun* 2016;52:4706-9. DOI
54. Evans AM, Strauss MJ, Corcos AR, et al. Two-dimensional polymers and polymerizations. *Chem Rev* 2022;122:442-564. DOI
55. Peng L, Guo Q, Song C, et al. Ultra-fast single-crystal polymerization of large-sized covalent organic frameworks. *Nat Commun* 2021;12:5077. DOI PubMed PMC
56. Yang H, Xu J, Cao H, Wu J, Zhao D. Recovery of homogeneous photocatalysts by covalent organic framework membranes. *Nat Commun* 2023;14:2726. DOI PubMed PMC
57. Zhan G, Cai ZF, Strutyński K, et al. Observing polymerization in 2D dynamic covalent polymers. *Nature* 2022;603:835-40. DOI
58. Khan NA, Zhang R, Wu H, et al. Solid-vapor interface engineered covalent organic framework membranes for molecular separation. *J Am Chem Soc* 2020;142:13450-8. DOI
59. Tang J, Liang Z, Qin H, et al. Large-area free-standing metalloporphyrin-based covalent organic framework films by liquid-air interfacial polymerization for oxygen electrocatalysis. *Angew Chem Int Ed* 2023;62:e202214449. DOI
60. Zhou D, Tan X, Wu H, Tian L, Li M. Synthesis of C-C bonded two-dimensional conjugated covalent organic framework films by suzuki polymerization on a liquid-liquid interface. *Angew Chem Int Ed* 2019;58:1376-81. DOI
61. Evans AM, Parent LR, Flanders NC, et al. Seeded growth of single-crystal two-dimensional covalent organic frameworks. *Science* 2018;361:52-7. DOI

62. Jin E, Li J, Geng K, et al. Designed synthesis of stable light-emitting two-dimensional sp^2 carbon-conjugated covalent organic frameworks. *Nat Commun* 2018;9:4143. DOI PubMed PMC
63. Wang S, Wang Q, Shao P, et al. Exfoliation of covalent organic frameworks into few-layer redox-active nanosheets as cathode materials for lithium-ion batteries. *J Am Chem Soc* 2017;139:4258-61. DOI
64. Liu J, Lyu P, Zhang Y, Nachtigall P, Xu Y. New layered triazine framework/exfoliated 2D polymer with superior sodium-storage properties. *Adv Mater* 2018:30. DOI PubMed
65. Bunck DN, Dichtel WR. Bulk synthesis of exfoliated two-dimensional polymers using hydrazone-linked covalent organic frameworks. *J Am Chem Soc* 2013;135:14952-5. DOI PubMed
66. Zhang Z, Xiao A, Yin C, Wang X, Shi X, Wang Y. Heterostructured two-dimensional covalent organic framework membranes for enhanced ion separation. *Chem Commun* 2022;58:7136-9. DOI
67. Feng X, Ding X, Chen L, et al. Two-dimensional artificial light-harvesting antennae with predesigned high-order structure and robust photosensitising activity. *Sci Rep* 2016;6:32944. DOI PubMed PMC
68. Lukose B, Kuc A, Heine T. The structure of layered covalent-organic frameworks. *Chemistry* 2011;17:2388-92. DOI PubMed
69. Yu F, Liu W, Ke SW, Kurmoo M, Zuo JL, Zhang Q. Electrochromic two-dimensional covalent organic framework with a reversible dark-to-transparent switch. *Nat Commun* 2020;11:5534. DOI PubMed PMC
70. Mahmood J, Ahmad I, Jung M, et al. Two-dimensional amine and hydroxy functionalized fused aromatic covalent organic framework. *Commun Chem* 2020;3:31. DOI PubMed PMC
71. Li RL, Yang A, Flanders NC, Yeung MT, Sheppard DT, Dichtel WR. Two-dimensional covalent organic framework solid solutions. *J Am Chem Soc* 2021;143:7081-7. DOI PubMed
72. Cao L, Chen IC, Li Z, et al. Switchable Na^+ and K^+ selectivity in an amino acid functionalized 2D covalent organic framework membrane. *Nat Commun* 2022;13:7894. DOI PubMed PMC
73. Wu X, Han X, Liu Y, Liu Y, Cui Y. Control interlayer stacking and chemical stability of two-dimensional covalent organic frameworks via steric tuning. *J Am Chem Soc* 2018;140:16124-33. DOI
74. Zhuang S, Lei L, Nunna B, Lee ES. New nitrogen-doped graphene/MOF-modified catalyst for fuel cell systems. *ECS Trans* 2016;72:149-54. DOI
75. Duresa LW, Kuo D, Bekena FT, Kebede WL. Simple room temperature synthesis of oxygen vacancy-rich and In-doped BiOBr nanosheet and its highly enhanced photocatalytic activity under visible-light irradiation. *J Phys Chem Solids* 2021;156:110132. DOI
76. Chen R, Wang Y, Ma Y, et al. Rational design of isostructural 2D porphyrin-based covalent organic frameworks for tunable photocatalytic hydrogen evolution. *Nat Commun* 2021;12:1354. DOI PubMed PMC
77. Evans AM, Bradshaw NP, Litchfield B, et al. High-sensitivity acoustic molecular sensors based on large-area, spray-coated 2D covalent organic frameworks. *Adv Mater* 2020;32:e2004205. DOI
78. Yu H, Wang J, Xie F, et al. A stack-guiding unit constructed 2D COF with improved charge carrier transport and versatile photocatalytic functions. *Chem Eng J* 2022;445:136713. DOI
79. Kim KH, Choi C, Choung S, et al. Continuous oxygen vacancy gradient in TiO_2 photoelectrodes by a photoelectrochemical-driven "self-purification" process. *Adv Energy Mater* 2022;12:2103495. DOI
80. Biswas S, Dey A, Rahimi FA, Barman S, Maji TK. Metal-free highly stable and crystalline covalent organic nanosheet for visible-light-driven selective solar fuel production in aqueous medium. *ACS Catal* 2023;13:5926-37. DOI
81. Lee SA, Yang JW, Lee TH, et al. Multifunctional nano-heterogeneous $Ni(OH)_2$/NiFe catalysts on silicon photoanode toward efficient water and urea oxidation. *Appl Catal B* 2022;317:121765. DOI
82. Bae S, Lee S, Ryu H, Lee W. Improvement of photoelectrochemical properties of CuO photoelectrode by Li doping. *Korean J Met Mater* 2022;60:577-86. DOI
83. Nguyen VH, Nguyen BS, Hu C, et al. Novel architecture titanium carbide ($Ti_3C_2T_x$) MXene cocatalysts toward photocatalytic hydrogen production: a mini-review. *Nanomaterials* 2020;10:602. DOI PubMed PMC
84. Do HH, Nguyen DLT, Nguyen XC, et al. Recent progress in TiO_2-based photocatalysts for hydrogen evolution reaction: a review. *Arab J Chem* 2020;13:3653-71. DOI
85. Nguyen V, Nguyen B, Jin Z, et al. Towards artificial photosynthesis: sustainable hydrogen utilization for photocatalytic reduction of CO_2 to high-value renewable fuels. *Chem Eng J* 2020;402:126184. DOI
86. Nguyen TP, Nguyen DLT, Nguyen VH, et al. Recent advances in TiO_2-based photocatalysts for reduction of CO_2 to fuels. *Nanomaterials* 2020;10:337. DOI PubMed PMC
87. Cho JH, Ma J, Kim SY. Toward high-efficiency photovoltaics-assisted electrochemical and photoelectrochemical CO_2 reduction: strategy and challenge. *Exploration* 2023;3:20230001. DOI PubMed PMC
88. Yang Y, Shen Y, Wang L, Song Y, Wang L. Three-dimensional porous carbon/covalent-organic framework films integrated electrode for electrochemical sensors. *J Electroanal Chem* 2019;855:113590. DOI
89. Zhu Y, Shao P, Hu L, et al. Construction of interlayer conjugated links in 2D covalent organic frameworks via topological polymerization. *J Am Chem Soc* 2021;143:7897-902. DOI
90. Zhao X, Pachfule P, Thomas A. Covalent organic frameworks (COFs) for electrochemical applications. *Chem Soc Rev* 2021;50:6871-913. DOI PubMed
91. Yang C, Mao C, Deng Q, Yang Y, Zhou Y, Zhang Y. One-Pot synthesis of flavones catalyzed by an Au-mediated covalent organic framework. *J Colloid Interface Sci* 2023;642:283-91. DOI PubMed

92. Li C, Yu G. Controllable synthesis and performance modulation of 2D covalent-organic frameworks. *Small* 2021;17:e2100918. DOI
93. Tang J, Su C, Shao Z. Covalent organic framework (COF)-based hybrids for electrocatalysis: recent advances and perspectives. *Small Methods* 2021;5:e2100945. DOI PubMed
94. Sun K, Xiao F, Yu B, He W. Photo-/electrocatalytic functionalization of quinoxalin-2(*1H*)-ones. *Chinese J Catal* 2021;42:1921-43. DOI
95. Liu C, Li H, Liu F, et al. Intrinsic activity of metal centers in metal-nitrogen-carbon single-atom catalysts for hydrogen peroxide synthesis. *J Am Chem Soc* 2020;142:21861-71. DOI
96. Liu Q, Li J, Wang J. Research of covalent organic frame materials based on porphyrin units. *J Incl Phenom Macrocycl Chem* 2019;95:1-15. DOI
97. Haase F, Lotsch BV. Solving the COF trilemma: towards crystalline, stable and functional covalent organic frameworks. *Chem Soc Rev* 2020;49:8469-500. DOI PubMed
98. An S, Li X, Shang S, et al. One-dimensional covalent organic frameworks for the $2e^-$ oxygen reduction reaction. *Angew Chem Int Ed* 2023;62:e202218742. DOI
99. Gao Z, Yu Z, Huang Y, et al. Flexible and robust bimetallic covalent organic frameworks for the reversible switching of electrocatalytic oxygen evolution activity. *J Mater Chem A* 2020;8:5907-12. DOI
100. Chang C, Wei Y, Kuo W. Free-standing CuS-ZnS decorated carbon nanotube films as immobilized photocatalysts for hydrogen production. *Int J Hydrog Energy* 2019;44:30553-62. DOI
101. Wang X, Sun L, Zhou W, Wu H, Deng W. Iron single-atom catalysts confined in covalent organic frameworks for efficient oxygen evolution reaction. *Cell Rep Phys Sci* 2022;3:100804. DOI
102. Qiu XF, Huang JR, Yu C, et al. A Stable and conductive covalent organic framework with isolated active sites for highly selective electroreduction of carbon dioxide to acetate. *Angew Chem Int Ed* 2022;61:e202206470. DOI
103. Yusran Y, Fang Q, Qiu S. Postsynthetic covalent modification in covalent organic frameworks. *Israel J Chem* 2018;58:971-84. DOI
104. Jin B, Cho Y, Park C, et al. A two-photon tandem black phosphorus quantum dot-sensitized $BiVO_4$ photoanode for solar water splitting. *Energy Environ Sci* 2022;15:672-9. DOI
105. Lee MG, Yang JW, Park H, et al. Crystal facet engineering of TiO_2 nanostructures for enhancing photoelectrochemical water splitting with $BiVO_4$ nanodots. *Nanomicro Lett* 2022;14:48. DOI PubMed PMC
106. Tian C, Liu R, Zhang Y, Yang W, Wang B. Ru-doped functional porous materials for electrocatalytic water splitting. *Nano Res* 2023. DOI
107. Bhunia S, Das SK, Jana R, et al. Electrochemical stimuli-driven facile metal-free hydrogen evolution from pyrene-porphyrin-based crystalline covalent organic framework. *ACS Appl Mater Interfaces* 2017;9:23843-51. DOI
108. Zhao Y, Li T, Gu J, et al. Covalent triazine frameworks based on different stacking model as electrocatalyst for hydrogen evolution. *Appl Surface Sci* 2023;618:156697. DOI
109. Ruidas S, Mohanty B, Bhanja P, et al. Metal-free triazine-based 2D covalent organic framework for efficient H_2 evolution by electrochemical water splitting. *ChemSusChem* 2021;14:5057-64. DOI
110. Halder S, Pradhan AK, Khan S, Chakraborty C. Generation of covalent organic framework-derived porous N-doped carbon nanosheets for highly efficient electrocatalytic hydrogen evolution. *Energy Adv* 2023;2:1713-23. DOI
111. Zhao Q, Chen S, Ren H, Chen C, Yang W. Ruthenium nanoparticles confined in covalent organic framework/reduced graphene oxide as electrocatalyst toward hydrogen evolution reaction in alkaline media. *Ind Eng Chem Res* 2021;60:11070-8. DOI
112. Maiti S, Chowdhury AR, Das AK. Electrochemically facile hydrogen evolution using ruthenium encapsulated two dimensional covalent organic framework (2D COF). *ChemNanoMat* 2020;6:99-106. DOI
113. Pan R, Wu J, Wang W, Cheng C, Liu X. Robust crystalline aromatic imide-linked two-dimensional covalent organic frameworks confining ruthenium nanoparticles as efficient hydrogen evolution electrocatalyst. *Colloids Surf A Physicochem Eng Asp* 2021;621:126511. DOI
114. Wang W, Zhang L, Gao C, et al. Covalent organic framework derived Mo_2C-$MoNi_4$ chainmail catalysts for hydrogen evolution. *Appl Surf Sci* 2023;627:157322. DOI
115. Xu Q, Tang Y, Zhang X, Oshima Y, Chen Q, Jiang D. Template conversion of covalent organic frameworks into 2D conducting nanocarbons for catalyzing oxygen reduction reaction. *Adv Mater* 2018;30:e1706330. DOI
116. Das SK, Kumar G, Das M, Dey RS. A 2D covalent organic framework as a metal-free electrode towards electrochemical oxygen reduction reaction. *Mater Today Proc* 2022;57:228-33. DOI
117. Zhang J, Zhao Z, Xia Z, Dai L. A metal-free bifunctional electrocatalyst for oxygen reduction and oxygen evolution reactions. *Nat Nanotechnol* 2015;10:444-52. DOI
118. Ji J, Zhang C, Qin S, Jin P. First-principles investigation of two-dimensional covalent-organic framework electrocatalysts for oxygen evolution/reduction and hydrogen evolution reactions. *Sustain Energy Fuels* 2021;5:5615-26. DOI
119. Tavakoli E, Kakekhani A, Kaviani S, et al. In situ bottom-up synthesis of porphyrin-based covalent organic frameworks. *J Am Chem Soc* 2019;141:19560-4. DOI
120. Li S, Gao Y, Li N, Ge L, Bu X, Feng P. Transition metal-based bimetallic MOFs and MOF-derived catalysts for electrochemical oxygen evolution reaction. *Energy Environ Sci* 2021;14:1897-927. DOI
121. Cai M, Ding S, Gibbons B, Yang X, Kessinger MC, Morris AJ. Nickel(II)-modified covalent-organic framework film for electrocatalytic oxidation of 5-hydroxymethylfurfural (HMF). *Chem Commun* 2020;56:14361-4. DOI PubMed

122. Lee SJ, Park YS. Effect of synthesis temperature on oxygen evolution reaction of cobalt-iron layered double hydroxide. *Korean J Met Mater* 2022;46:326-9. DOI
123. Xu J, Tang W, Yang C, et al. A highly conductive COF@CNT electrocatalyst boosting polysulfide conversion for Li-S chemistry. *ACS Energy Lett* 2021;6:3053-62. DOI
124. Zhang Z, Wang W, Wang X, Zhang L, Cheng C, Liu X. Ladder-type π-conjugated metallophthalocyanine covalent organic frameworks with boosted oxygen reduction reaction activity and durability for zinc-air batteries. *Chem Eng J* 2022;435:133872. DOI
125. Hao Q, Zhao C, Sun B, et al. Confined synthesis of two-dimensional covalent organic framework thin films within superspreading water layer. *J Am Chem Soc* 2018;140:12152-8. DOI
126. Yan Y, Qin H, Ding D, et al. Ultrathin cage-based covalent organic framework nanosheets as precursor for pyrolysis-free oxygen evolution reaction electrocatalyst. *ChemNanoMat* 2022;8:e202200305. DOI
127. Yang C, Yang Z, Dong H, et al. Theory-driven design and targeting synthesis of a highly-conjugated basal-plane 2D covalent organic framework for metal-free electrocatalytic OER. *ACS Energy Lett* 2019;4:2251-8. DOI
128. Cui J, Liu J, Wang C, et al. Efficient electrocatalytic water oxidation by using the hierarchical 1D/2D structural nanohybrid of CoCu-based zeolitic imidazolate framework nanosheets and graphdiyne nanowires. *Electrochimica Acta* 2020;334:135577. DOI
129. Zhang R, Liu W, Zhang F, Yang Z, Zhang G, Zeng XC. COF-C4N nanosheets with uniformly anchored single metal sites for electrocatalytic OER: from theoretical screening to target synthesis. *Appl Catal B* 2023;325:122366. DOI
130. Martínez-Fernández M, Martínez-periñán E, Martínez JI, et al. Evaluation of the oxygen reduction reaction electrocatalytic activity of postsynthetically modified covalent organic frameworks. *ACS Sustain Chem Eng* 2023;11:1763-73. DOI
131. Chang J, Li C, Wang X, et al. Quasi-three-dimensional cyclotriphosphazene-based covalent organic framework nanosheet for efficient oxygen reduction. *Nanomicro Lett* 2023;15:159. DOI PubMed PMC
132. García-Arroyo P, Martínez-periñán E, Cabrera-trujillo JJ, et al. Pyrenetetraone-based covalent organic framework as an effective electrocatalyst for oxygen reduction reaction. *Nano Res* 2022;15:3907-12. DOI
133. Kumar A, Ubaidullah M, Pandit B, Yasin G, Gupta RK, Zhang G. Fe-phthalocyanine derived highly conjugated 2D covalent organic framework as superior electrocatalyst for oxygen reduction reaction. *Discov Nano* 2023;18:109. DOI PubMed PMC
134. Chi S, Chen Q, Zhao S, et al. Three-dimensional porphyrinic covalent organic frameworks for highly efficient electroreduction of carbon dioxide. *J Mater Chem A* 2022;10:4653-9. DOI
135. Lei K, Yu Xia B. Electrocatalytic CO_2 reduction: from discrete molecular catalysts to their integrated catalytic materials. *Chemistry* 2022;28:e202200141. DOI PubMed
136. Nie W, Tarnopol DE, Mccrory CC. The effect of extended conjugation on electrocatalytic CO_2 reduction by molecular catalysts and macromolecular structures. *Curr Opin Electrochem* 2021;28:100716. DOI
137. Zhang M, Lu M, Yang M, et al. Ultrafine Cu nanoclusters confined within covalent organic frameworks for efficient electroreduction of CO_2 to CH_4 by synergistic strategy. *eScience* 2023;3:100116. DOI
138. Xu K, Dai Y, Ye B, Wang H. Two dimensional covalent organic framework materials for chemical fixation of carbon dioxide: excellent repeatability and high selectivity. *Dalton Trans* 2017;46:10780-5. DOI PubMed
139. Yang YL, Wang YR, Dong LZ, et al. A honeycomb-like porous crystalline hetero-electrocatalyst for efficient electrocatalytic CO_2 reduction. *Adv Mater* 2022;34:e2206706. DOI
140. Zhao Q, Wang Y, Li M, et al. Organic frameworks confined Cu single atoms and nanoclusters for tandem electrocatalytic CO_2 reduction to methane. *SmartMat* 2022;3:183-93. DOI
141. Cho JH, Lee C, Hong SH, et al. Transition metal ion doping on ZIF-8 enhances the electrochemical CO_2 reduction reaction. *Adv Mater* 2023;35:e2208224. DOI
142. Kim S, Kim KH, Oh C, Zhang K, Park JH. Artificial photosynthesis for high-value-added chemicals: old material, new opportunity. *Carbon Energy* 2022;4:21-44. DOI
143. Wu Q, Mao MJ, Wu QJ, Liang J, Huang YB, Cao R. Construction of donor-acceptor heterojunctions in covalent organic framework for enhanced CO_2 electroreduction. *Small* 2021;17:e2004933. DOI PubMed
144. Zhu HJ, Lu M, Wang YR, et al. Efficient electron transmission in covalent organic framework nanosheets for highly active electrocatalytic carbon dioxide reduction. *Nat Commun* 2020;11:497. DOI PubMed PMC
145. Lu Y, Zhang J, Wei W, Ma DD, Wu XT, Zhu QL. Efficient carbon dioxide electroreduction over ultrathin covalent organic framework nanolayers with isolated cobalt porphyrin units. *ACS Appl Mater Interfaces* 2020;12:37986-92. DOI
146. Zhang MD, Si DH, Yi JD, Zhao SS, Huang YB, Cao R. Conductive phthalocyanine-based covalent organic framework for highly efficient electroreduction of carbon dioxide. *Small* 2020;16:2005254. DOI PubMed
147. Miao Q, Lu C, Xu Q, et al. CoN_2O_2 sites in carbon nanosheets by template-pyrolysis of COFs for CO_2RR. *Chem Eng J* 2022;450:138427. DOI
148. Liu G, Li X, Liu M, et al. Dimensional engineering of covalent organic frameworks derived carbons for electrocatalytic carbon dioxide reduction. *SusMat* 2023;3:834-42. DOI